universität wien

MASTERARBEIT / MASTER'S THESIS

Titel der Masterarbeit / Title of the Master's Thesis

„Protein-protein interactions between human cytomegalovirus tegument proteins and human protein phosphatase 1“

verfasst von / submitted by

Sanja Marinkov

angestrebter akademischer Grad / in partial fulfilment of the requirements for the degree of

Master of Science (MSc)

Wien, 2021/ Vienna, 2021

Studienkennzahl lt. Studienblatt / degree programme code as it appears on the student record sheet:	A 066 877
Studienrichtung lt. Studienblatt / degree programme as it appears on the student record sheet:	Masterstudium Genetik und Entwicklungsbiologie
Betreut von / Supervisor:	Assoc. Prof. Priv.-Doz. Dr. Christoph Steininger

Acknowledgement

Frist, I would like to thank Assoc.-Prof. Dr. Christoph Steininger for giving me the opportunity to be a part of his research group and for the support during this project.

A special thank goes to my supervisor, Carmen Stecher, who provided me invaluable advice, support, and patience during my thesis. I am grateful for your immense knowledge and help, which meant a lot to me. You are a great supervisor and a wonderful person, it has been a pleasure and a privilege working with you.

I would also like to thank all other members of the lab group, Ceren Bilgilier, Jakob Thannesberger, Lucia Mayr-Harting, Marie Theres-Kastner and Victoria Podgorzak. I really enjoyed working with you in the lab as well as the time outside of the lab.

Finally, I would like to thank my boyfriend, Milovan Stojanovic, for providing me support and continuous encouragement throughout my years of study and through the process of writing this thesis.

Contents

Abstract

Human cytomegalovirus (HCMV) is a widespread pathogen causing life-long infection and serious disease in immunocompromised patients. Previous research has shown that HCMV carries the human Ser/Thr Protein Phosphatase 1 (PP1), which it captures from infected cells, in its own tegument. The molecular mechanisms of this phosphatase incorporation into the viral particle and their biological consequences are still unclear.

The aim of this study was to identify HCMV tegument proteins that bind to PP1. Previous research of our group identified UL32 as a candidate of PP1 binding via a short RVxF motif. By using a mutational approach and mammalian 2hybrid (M2H) assays, we could show that the observed weak signal is likely not a specific, RVxF-mediated interaction. We further determined that full-length proteins are more suited to discover PP1 interactors compared to peptides when using the M2H system. However, we did not obtain evidence of PP1 interaction with the HCMV proteins UL24, UL32, UL38 and UL82 on the whole protein level. Multiple Mass spectrometry datasets indicate that HCMV virions contain multiple human proteins, some of which are potential PP1 interactors. However, no evidence of direct interaction with 4 candidate proteins was found using M2H or preliminary co-immunoprecipitation (Co-IP) assays.

Finally, we established a Co-IP protocol for interaction of His-tagged PP1 with HA-SDS22 and other potential PP1 binders. This method will be useful in the investigation of PP1 interactors, which will contribute to identify the HCMV binding partner of PP1 and help understand the mechanism of PP1 incorporation into the HCMV tegument.

1 Introduction

1.1 Human Cytomegalovirus

Human cytomegalovirus (HCMV), also referred to as human herpesvirus 5 (HHV-5), is a member of the *Betaherpesvirinae* sub-family of *Herpesviridae* [1]. It is a widespread pathogen and infects between 50 and 85% of adults by the age of 40. HCMV can cause significant morbidity and mortality in immunocompromised hosts whose immune systems are weakened, such as organ transplant or AIDS patients. Symptoms of these individuals are spiking fever, leucopenia (i.e. a decrease in white blood cells), malaise, hepatitis, pneumonia, gastrointestinal disease and retinitis [2]. Immunocompetent individuals with a strong immune response mostly display no symptoms of infection. After primary infection, HCMV can persist for the lifetime of the host by its ability to establish a latent infection in the absence of virion production [3]. Latency is not a completely quiescent state but is specified by limited viral gene expression. Immunosuppression of the carrier leads to the reactivation of the latent infection and replication in a lytic cycle of infection [4].

The virus is easily transmitted by the direct contact of mucous membranes with infectious body fluids, such as nasal secretions, saliva, tears, urine and genital secretions. After infection, the virus starts to replicate in the epithelial cells at the site of entry and spreads to various organs and cell types, such as endothelial cells, fibroblasts, smooth muscle cells, monocytes and macrophages [5], [6]. HCMV is the most common congenital viral infection, which occurs in 0.3% to 2.4% of all live births in the developed world. Mothers infected with HCMV can transmit the virus to their child by close contact (via contaminated blood, urine and secretions), prenatally through placenta and postnatally through breast milk [7]. Pre-existing immunity of the mother does not prevent infection of the fetus *per se*, but in most cases primary infection of the mother causes the harm of the offspring [8]. Congenital HCMV infection can lead to consequences such as thrombocytopenia, central nervous system and ocular disease, sensorineural hearing loss and significant subsequent mortality rates. Additionally, the severity of infection probably depends on timing during pregnancy. More severe sequelae are related to infection earlier in the pregnancy [9].

Human cytomegalovirus causes several serious diseases in immunocompromised individuals and so far, there is no effective vaccine against HCMV [10]. HCMV infection is treated by using drugs which inhibit the viral replication but cannot remove the virus from the organism. Ganciclovir, foscarnet, letermovir and cidofovir are common drugs used in HCMV therapy. These drugs can improve the quality of life of

patients suffering from HCMV, but they are still not efficient enough due to high toxicity, poor bioavailability and the development of virus resistance [2]. Since treatment options for HCMV infection are scarce, there are intense ongoing efforts for the identification of proteins and processes that could be targeted by novel antiviral treatments [2], [10].

1.2 HCMV structure

HCMV is the largest known human herpesvirus with a diameter of 200 to 300 nanometers [11]. The virus has a double-stranded DNA genome (230-240 kbp), which encodes at least 165 genes, four non-coding RNAs and 14 miRNAs [12]. The viral DNA is enclosed by an icosahedral capsid. The capsid is covered by the tegument, a layer mostly composed of proteins, but it may contain some RNAs. The tegument is surrounded by an envelope composed of glycoproteins (**Figure 1**). The viral envelope initiates the contact with different host cells and is responsible for the broad tropism of HCMV [13].

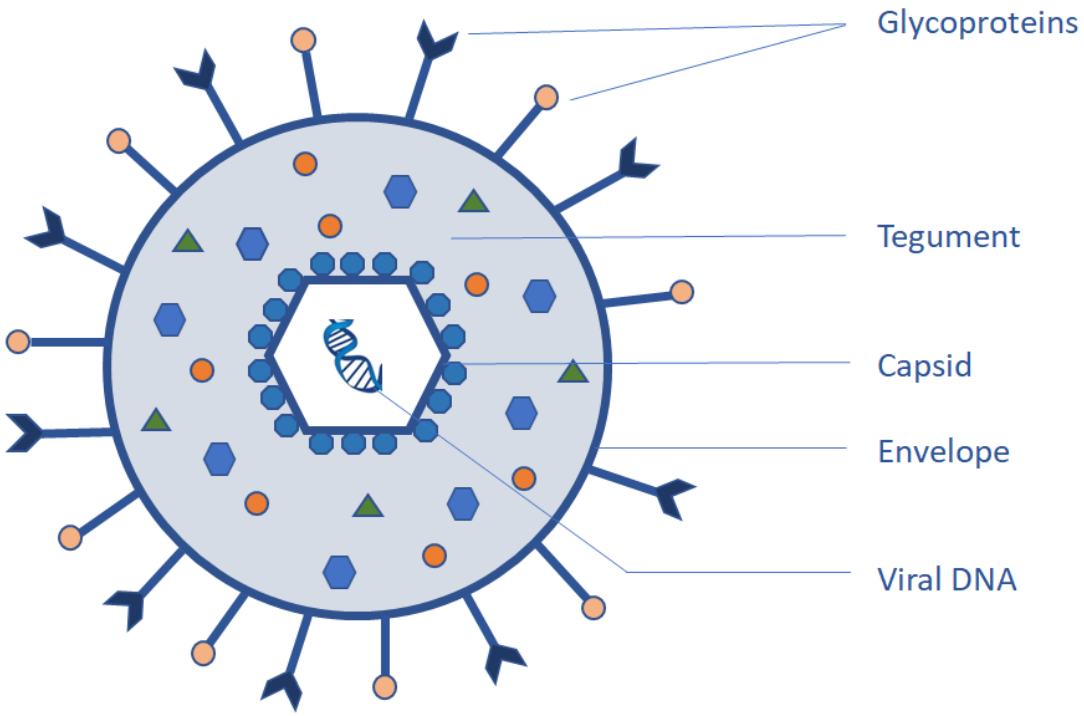

Figure 1) Schema of the HCMV particle. The viral DNA is enclosed by a capsid which is surrounded by the viral tegument and envelope carrying glycoproteins. Adapted from Kalejta, 2008 [14].

1.3 HCMV life cycle

HCMV is characterized by a wide cell tropism within its human host. The cellular epigenetic mechanisms play an important role in the regulation of viral gene expression and influence the type of HCMV infection [14].

The viral envelope contains glycoproteins that mediate the fusion with host cells. After fusion of the two membranes, the tegument proteins together with the DNA containing capsid are released into the cell [15]. After viral entry, HCMV initiates lytic infection by starting its gene expression in the following order: first immediate-early (IE), early (E) and finally late (L) gene expression. The immediate-early genes regulate cellular DNA synthesis or alter the host organism's immune response to the virus in order to enable an optimal environment for virus replication [16]. Some of the crucial IE genes are IE1 and IE2 (also called pp72 and pp86), which are involved in the downregulation of the IFN-α/β-mediated signaling response and inhibition of apoptosis [17]. The early gene products are essential for viral DNA replication and their expression starts approximately 8 hours post infection (h.p.i.). Some early genes are included in cleavage and packaging of the viral genome. The viral replication is prolonged and tightly regulated, so that viral late gene expression and progeny occur after 2 to 3 days of infection [18]. The late gene expression is strictly dependent on viral DNA replication and is essential for the assembly and egress of new viral particles [19].

In contrast to the lytic cycle, during latent infection the gene expression is decreased, and the assembly and egress of new viral progeny is inhibited. Latent infection can occur in haematopoietic precursors in the bone marrow, including monocytes and dendritic cells. Latent infection can reactivate into a lytic cycle by immunosuppressive cues, leading to the development of disease and viral spreading [2], [20]. The cellular differentiation state affects the maintenance of latency and reactivation. The differentiation of haematopoietic progenitors can influence HCMV infection: monocytes appear to maintain latent infection, while activated macrophages support reactivation and active replication [21].

HCMV infected cells can also produce noninfectious enveloped particles and so called dense bodies. Noninfectious enveloped particles are similar to infectious virions and contain envelope, tegument and capsid proteins but no double-stranded viral genome. On the other hand, dense bodies are enveloped tegument proteins that lack capsids as well as viral genomes [15].

1.4 HCMV tegument proteins

The tegument is a layer between the nucleocapsid and outer envelope, generally unstructured or amorphous. The tegument layer in HCMV consists of at least 30 proteins, ranging in size from 11 to more than 200 kDa [22]. The tegument proteins are included in all stages of the viral life cycle, as e.g. viral entry, gene expression, immune evasion, assembly and egress [13], [15]. Hence, HCMV tegument proteins have been proposed as potential therapeutic targets. Upon infection, all tegument proteins are released into the host cell [23]. Some of the tegument proteins remain in the cytoplasm, while others migrate to the cell nucleus. The proteins which migrate to the nucleus are mostly tightly associated with the capsid and mediate the delivery of capsid with DNA to the cell nucleus, while other proteins like pp65 and pp71 migrate independently [15]. After viral replication, capsid formation and DNA packaging occurs in the nucleus. Then, the capsid with a primary envelope migrates through the outer nuclear membrane into the cytoplasm. Finally, the virus is enveloped into Golgi apparatus-derived vesicles and when these vesicles fuse with the cell membrane, the enveloped virion is released [15], [24].

A reactivating virus cannot make use of the pre-formed tegument proteins, which represents one of the important differences between primary infection and reactivation [13].

1.4.1 pp150 (UL32)

pp150, encoded by the UL32 gene, is the second most abundant tegument protein behind pp65. There are approximately 1500 copies of pp150 in a viral particle [15]. The phosphoprotein pp150 is synthesized in equivalent amounts by wild-type as well as laboratory strains and is one of the most antigenic viral components in humans [25]. pp150 is connected with the capsid via its amino terminus, and is required during HCMV infection [15].

At early times of infection, pp150 localizes to the nucleus and stabilizes the DNA-containing capsids as they progress from the nucleus to the cytoplasmic assembly complex (AC) [23]. The DNA-containing capsid migrates to the AC using dynein and the microtubules that radiate from a microtubule organizing center (MTOC), which is the place of the AC formation [26]. Host proteins can contribute to the proper localization of viral proteins. In the cells, the protein Bicaudal D1 (BicD1) links Rab6 to dynein. The small GTPase Rab6 interacts with pp150 and mediates the capsid migration to the AC [27]. It has been shown that inhibition of Rab6 blocks the intracellular trafficking of pp150 and reduces virus production without affecting the formation of the AC [28].

Additionally, pp150 is included also in the regulation of IE gene expression in dependence of the cell cycle of infected cells [29]. The lytic cycle of HCMV starts only in G_1 phase of the cell cycle. HCMV can infect cells in the S/G_2 phase, but immediate-early (IE) gene expression is blocked [30]. The viral replication depends on metabolites and replication factors from the host cell. Hence, the cells in S phase and in mitosis would negatively affect viral replication, which needs the host machinery to achieve maximum replication. Additionally, the structural changes occurring in mitosis such as the nuclear envelope breakdown could disrupt HCMV replication [31]. In order to replicate successfully, HCMV expresses pp150 to regulate IE genes in S/G_2 phase of the cell cycle and UL21, which maintains the G_1 cell cycle state until the release of virus progeny [31]. It has been detected that the interaction between cellular cyclin A2 and protein pp150 is required for the inhibition of viral IE gene expression in cells during the S/G_2 phase. Thereby, pp150 ensures the right timing of viral gene expression during G_1. Additionally, the unphosphorylated pp150 is more sensitive to cyclin A2 and there is a possibility that phosphatases like PP1 and PP2A might induce the dephosphorylation of pp150 and thus support the regulation of IE gene expression [29]. In contrast to HCMV, chimpanzee CMV (CCMV) and murine CMV (MCMV) express IE genes with the same efficiency in the G0/G1 and S/G2 cell cycle. The difference between these species is probably a result of the different structure of pp150. The N-terminus is conserved across all species and is bound to the viral capsid, while the C-terminus is highly divergent in size and sequence. Only HCMV contains RXL/Cy motifs for the recognition of cyclin A2. This finding indicates that the cyclin A2–pp150 interaction plays an important role in the control of gene expression in HCMV and might contribute to the selection of host cells suitable for latent infection [29].

1.4.2 UL38

UL38 is a tegument protein that prevents premature cell death during HCMV infection [32]. Throughout HCMV infection, iron uptake is increased. However, the increased iron absorption must be regulated in order to prevent cell death caused by excess iron in the cell [33]. Ferritin is responsible for iron storage and homeostasis. In the absence of iron, ferritin is degraded in the lysosome, releasing iron in the cells. Uncontrolled degradation of ferritin results in apoptosis [34]. During HCMV infection, UL38 interacts with the ubiquitin-specific protease 24 (USP24), which mediates the autophagic ferritin degradation in lysosomes. This association inhibits the ferritin degradation and thus cell death [33].

HCMV also induces the release of Ca^{2+} from the ER to the cytosol and in this way impacts the ER function during infection [35]. In order to stabilize the ER function, the unfolded protein response (UPR) is activated to reduce stress or induce cell death. However, UL38 interferes with UPR and mediates the

phosphorylation of the α subunit of eukaryotic initiation factor 2 (eIF-2α) by PERK leading to the translation of the activating transcriptional factor 4 (ATF4) [36]. ATF4 activates the genes involved in oxidative stress as well as amino acid synthesis and thus prevents the cell death [37].

Considering that viruses do not encode translation initiation factors themselves, they depend on their hosts to increase translation-factor levels critical for their replication [38]. Under metabolically stressful conditions, the mammalian target of rapamycin complex 1 (mTORC1) is inhibited, which is the most important factor in the regulation of cellular macromolecule synthesis. However, during HCMV infection, host protein synthesis is not suppressed as it is the case with most viruses. UL38 interacts with a negative regulator of mTORC1, tuberous sclerosis protein 2 (TSC2) and prevents the mTORC1 inhibition. The active mTORC1 phosphorylates and inactivates a translation suppressor, eukaryotic translation initiation factor 4E binding protein 1 (4E-BP1), which prevents cap-dependent protein translation [35]. Additionally, UL38 recruits and accumulates translational factors by regulating poly(A) binding protein (PABA), which enhances the assembly of eukaryotic translation initiation factor 4F (eIF4F) [38].

Taken all together, UL38 is an important tegument protein in the inhibition of the apoptosis as well as in the reduction of metabolic stress during HCMV infection.

1.4.3 pp71 (UL82)

The tegument protein pp71 is encoded by the UL82 gene. pp71 is a phosphoprotein which migrates to the nucleus immediately after infection. It plays a role in the activation of the major immediate early promoter and viral gene expression [39]. HCMV infection with deleted pp71 results in the decreased production of viral progeny after infection, indicating that pp71 is important for HCMV replication [39]. pp71 activates gene expression by binding to the cellular protein Daxx, inducing its degradation. Daxx recruits histone deacetylases (HDACs) to the viral major IE promoters (MIEP), leading to transcriptional repression [15]. It has been shown that Daxx is required for the repression of IE genes and the establishment of latent infection. These findings indicate that the degradation of Daxx by pp71 can be essential to determine whether the lytic cycle will be initiated or latency will be established [15].

The expression of pp71 can affect the cell cycle in order to pave the way for efficient HCMV replication. pp71 induces quiescent cells to re-enter the cell cycle and accumulates them in late G1 phase, without inducing apoptosis. pp71 binds to hypophosphorylated Rb protein and promotes its degradation. This way, the interaction between Rb protein and the E2F transcription factor is prevented, as well as the

suppression of the transcription from promoters that are activated by E2F [40]. The genes activated by E2F are involved in the progression into the S phase and they can contribute to viral DNA replication [15]. pp71 leads to the push of the cell cycle into the G1 phase, but in an Rb-independent manner [40].

pp71 is also involved in the evasion of host antiviral responses by negatively regulating STING mediated signaling [41]. In the cell, foreign doubled-stranded DNA is recognized by the cGAS-STING pathway. If cGAS (cyclic GMP-CMP synthase) binds to cytosolic dsDNA, this leads to a conformational change in the active site, resulting in the synthesis of cyclic GMP-AMP (cGAMP). When cGAMP is released as a second messenger, it binds to the ER-membrane adaptor STING and activates it. The activated STING translocates from the ER to the Golgi apparatus, where it recruits and activates the TANK binding kinase 1 (TBK1). TBK1 phosphorylates the interferon regulatory factor 3 (IRF3), which then dimerizes and travels into the nucleus to activate several antiviral genes, such as e.g. type I interferons [42]. It has been shown that pp71 can affect the cGAS-STING pathway by two different ways. pp71 interacts with STING and disrupts the STING-iRhom2-TRAPb translocation complex formed at the ER, inhibiting its translocation from the ER to the Golgi apparatus. Additionally, pp71 can inhibit the recruitment of TBK1 and IRF3 to the STING complex and thereby suppress antiviral gene expression. Hence, pp71 is one of the tegument proteins important in the evasion from the host immune system [41].

Finally, pp71 can decrease the accumulation of cell surface MHC class I complexes, by delaying their transport from the ER or cis-Golgi apparatus [43].

1.4.4 pp65 (UL83)

pp65 is the most abundant HCMV tegument protein and is responsible for evading the host cell immune response during HCMV infection. pp65 is a target of both humoral and cellular (CD4 and CD8 T-cell) immunity and additionally, it serves as the dominant target antigen of cytotoxic T lymphocytes (CTL) [15]. CTLs are responsible for the recognition of viral peptides presented at the cell surface in the context of major histocompatibility complex (MHC) class I molecules. However, HCMV developed several mechanism to avoid CTL recognition [44]. For example, pp65 induces the phosphorylation of viral immediate-early proteins, preventing their presentation via MHC class I molecules [2].

Further, pp65 contributes to the escape of immune recognition by binding to the NKp30 activating receptor, preventing the killing of infected cells [45]. The NKp30 receptor is located at natural killer (NK) cells, which can discriminate between normal and stressed cells. Additionally, the NK cells are able to recognize and kill stressed cells in the absence of antibodies and MHC, providing a much faster immune

reaction compared to adaptive immunity [46]. The pp65 protein acts as a ligand for the receptor NKp30 and induces the dissociation of the ζ-chain from NKp30, leading to a general inhibition of NK cells to kill the virus-infected cells [45].

IFN-α/β are multifunctional cytokines and are produced in the response to viral infection. Several transcription factors can be involved in the regulation of IFN genes, such as NF-κB, AP-1 and IRF-3 [47]. IRF-3 is considered to be most important in the regulation of IFN-α/β response. Upon infection, IRF-3 is hyperphosphorylated and travels into the nucleus, where it activates the transcription of IFN genes [48]. It has been shown that pp65 has an impact on the interferon response, inhibiting the activation of IRF-3 within early times after infection. The mechanisms of IRF-3 inhibition by pp65 are still unknown. There are assumptions that pp65 may promote IRF-3 dephosphorylation or may block the cell kinases IKKε and TBK1 and thereby prevent IRF-3 phosphorylation [49].

pp65 can interact with cellular as well as viral proteins. The incorporation of the cellular Polo-like kinase 1 (Plk1) into virus particles is dependent the interaction with pp65. Also, it is known, that pp65 interacts with pUL97, which is likely required for the nuclear distribution of pp65 [50].

pp65 is very important for the modulation of the immune response, but the detailed mechanisms behind it are still unknown. It is also necessary to investigate if tegument-delivered proteins or newly synthesized proteins are major immune regulators [15].

The tegument proteins are involved in all stages of the HCMV life cycle, which shows how essential they are for HCMV. The assembly of the virion is a complex process, which involves many protein-protein interactions. The tegument proteins interact with viral as well as with cellular proteins [15]. The identification of these interactions will help to understand the biology of HCMV and the roles of tegument proteins. The HCMV tegument layer also contains cellular RNAs and their packaging is probably mediated through nonspecific interactions with HCMV proteins [51]. Beside RNA, around 70 human proteins are incorporated into the HCMV tegument [52]. Among these human proteins, the cellular phosphatases PP1 and PP2A were detected in the virion, suggesting the possibility of tegument protein post-translational modifications [53]. It is already known that HCMV infection upregulates PP1 and PP2A protein levels and their activity in the host cell, indicating that these phosphatases may play an important role for the life cycle of HCMV [54]. However, the molecular mechanism of their incorporation in HCMV tegument is still unknown.

1.5 Protein phosphatase 1 (PP1)

Different extracellular signals affect the intracellular transduction systems, resulting in the emergence of a specific biological response. A major role in cellular transduction systems is assumed by proteins. The balance between activation and deactivation of proteins in signaling pathways is tightly regulated through phosphorylation by kinases and through dephosphorylation induced by phosphatases [55]. The protein phosphatases are classified into 3 families: the phosphoprotein phosphatase (PPP) family, the metallo-dependent protein phosphatase (PPM) family, and the protein-tyrosine phosphatase (PTP) family. The PPP family includes the serine / threonine phosphatases (Ser/Thr phosphatases) PP1, PP2A, PP2B, PP4, PP6, PP5 and PP7 [56]. PP1 and PP2A are the most ubiquitous and abundant serine/threonine phosphatases in eukaryotic cells and are essential in the regulation of various cellular functions [57]. It is estimated that they are responsible for 90% of all Ser/Thr dephosphorylation events in a eukaryotic cell [58].

The serine/threonine phosphatase PP1 acts as a holoenzyme, containing a catalytic subunit (PP1C) and a regulatory subunit [59]. In mammalian cells there are four isoforms of the PP1 catalytic subunit (~38kDa), encoded by three different genes. PP1Cα is encoded by *PPP1CA*, PP1Cβ/δ by *PPP1CB* and the two splice variants PP1γ1 and PP1γ2 by *PPP1CC*. The similarity between these isoforms is about 90%, mostly differences are found in their N- and C-terminal domains [60]. PP1α, PP1β/δ and PP1γ1 are expressed in all cells and can be localized in the cytoplasm as well as in the nucleus [61]. PP1γ2 is expressed only in the testis and plays an important role in spermatogenesis [62].

In the cells, the catalytic subunit of PP1 does not occur alone, but is always in a complex with a regulatory protein [63]. So far, more than 200 PP1 regulatory proteins have been identified. Among these PP1 regulators there are also PP1 inhibitors, such as inhibitor-2 and DARPP-32, which are required for regulating PP1 activity. The association with regulatory proteins allows PP1 to target different cellular substrates and to change subcellular location [60]. Considering that PP1 targets a high number of substrates, PP1 is involved in many biological processes such as cell division, apoptosis, glycogen metabolism or protein synthesis [63]. Hence, it is not surprising that any inactivation or mutation of PP1 can indicate human pathologies such as cancer, heart disease or memory loss [64].

1.6 Structure of the PP1 holoenzyme

In mammalian cells there is a huge difference between the number of cellular serine/threonine kinases versus the number of opposing phosphatases. Around 400 proteins act as Ser/Thr kinases, while only 40

proteins as Ser/Thr phosphatases [65]. Therefore, Ser/Thr phosphatases have to interact with thousands of substrates. In order to achieve specificity, Ser/Thr phosphatases form holoenzymes with regulatory proteins. The different holoenzymes formed by Ser/Thr phosphatases show similar diversity as Ser/Thr kinases [63].

The catalytic subunit of PP1 (PP1c) is folded into a central β-sandwich that excludes the C terminal and the extreme N terminal region. In the active site of PP1c there are two metal ions, Zn^{2+} and Fe^{2+}, which are important for the hydrolysis of the phosphate group from substrates [63]. PP1c can be bound by one of more than 200 PP1 regulators, which determine its specific subcellular localization and substrate [60]. The interaction between PP1c and a regulator is allowed via one or more short linear motifs (SLiMs; ~4–8 residues). SLiM are mostly degenerate and flanked by unconserved stretches [66]. The majority of PP1 regulators contain the RVxF motif, which is 20 Å away from the catalytic site. Additionally, the SILK or MyPhoNE are less abundant motifs, but can also mediate the interaction with PP1 [67].

The binding of PP1 regulators via short motifs does not lead to a conformational change of PP1, and it has no impact on the metal ions in the active site [66]. Hence, more work is required to understand the mechanism of PP1 regulation as well as to find undiscovered protein-protein interactions in the PP1 interactome.

1.7 PP1-binding motifs

Over 200 PP1-interactors bind to PP1 catalytic subunits via multiple docking motifs as RVxF, SpiDoc, SILK, MyPhoNE, ΦΦ [68].

The RVxF motif is the most abundant PP1-binding motif, which occurs in 90% of PP1 regulators [68]. The RVxF motif acts as an anchor for PP1 recruitment. It increases the local concentration of PP1, resulting in secondary interactions that regulate the activity or substrate specificity of the phosphatase [67], [68]. The consensus sequence for the RVxF motif is [RK]-$X_{0–1}$-[VI]-{P}-[FW], where *X* can be any residue and {P} any residue except proline. Mutation of the RVXF decreases the affinity of an interactor to PP1 [69]. The RVXF motif can be required for the cooperative binding of other motifs, e.g. in interaction between the myosin targeting protein Mypt1 and PP1 [70].

The SILK motif with the consensus sequence [GS]-I-L-[KR]-{DE}, (where {DE} can be any amino acid except aspartic acid or glutamic acid [67]), occurs only in seven known PP1 regulators [68]. The SILK motif is e.g. found in Inhibitor-2 and is necessary for the PP1 inhibition. Additionally, the substitution of

the RVxF motif of NIPP1 by a SILK motif, can mediate the interaction with PP1. These findings indicate that SILK and RVxF motifs are equally potent PP1 binders [67]. In all proteins containing the SILK motif, it occurs always in combination with the RVxF motif and is located N-terminally to it [67]. The importance of "SILK" for PP1 binding seems to depend on the individual PP1 interactor. For example, a mutation of the SILK motif in SIPP1, a PP1 binding splicing factor, leads to the inhibition of the PP1:SIPP1 interaction, while a mutation of the SILK motif in Fam130A1 has almost no impact on the protein-protein interaction [67].

The MyPhoNE (myosin phosphatase N-terminal element) motif is also capable to mediate the binding of PP1 but is less abundant in PP1 regulators. There are only six known PP1 regulators with this motif [68]. Its consensus sequence is R x x Q V/I/L K/R x Y/W, where x can be any residue. Similar to SILK, MyPhoNE is always in combination with the RVxF motif and is located N-terminally to it [65]. The MyPhoNE motif found in MYPT1 mediates the interaction with PP1 via hydrophobic and electrostatic residues and might contribute to substrate selection [71].

The most recently identified motif is called ϕϕ motif. This motif is found in addition to the RVxF motif and defined by two hydrophobic residues that bind a hydrophobic pocket in PP1 [72]. It was found, that 43 PP1 interactors contain a RVxF-ΦΦ or RVxF-ΦΦ-R motif. Some of them are PNUTS, GADD34 and NIPP1 [72].

In addition to these three motifs, known PP1 binding motifs comprise the "SpiDoC" motif found in the spinophilin protein and the "IDoHA" motif found in the PP1 inhibitor-2 [68].

1.8 PP1 regulators

1.8.1 GADD34

The growth-arrest- and DNA damage-induced transcript 34 (GADD34), encoded by the *PPP1R15B* gene in mammalian cells, binds to PP1 via the two PP1-anchoring motifs RVxF and ϕϕ [73]. GADD34 (in the complex with PP1) mediates the dephosphorylation of the eukaryotic translation initiation factor 2α (eIF2α) [73]. Under stress conditions, such as nutrient deprivation or heat shock, eIF2α is activated by the phosphorylation by the cellular kinases GCN2, PERK, PKR, or HRI, resulting in the repression of protein synthesis. However, the transcription factors ATF4 and CHOP are expressed and activate the expression of GADD34 [74]. As the stress decreases, GADD34 binds to PP1 and mediates the dephosphorylation of eIF2α by PP1, leading to normal protein synthesis [73].

Additionally, the holoenzyme PP1:GADD34 is involved in TGF-β signaling, that regulates cell fate by controlling proliferation, differentiation and apoptosis [75]. Smad7 interacts with the holoenzyme PP1:GADD34 and mediates the dephosphorylation of TGF type I receptor, down-regulating the TGF signaling pathway [75].

1.8.2 SDS22

SDS22 (suppressor of Dis2 mutant 2) is one of the most conserved PP1 regulators [76], [77]. Interestingly, SDS22 binds to PP1 by twelve leucine-rich repeats (LRRs), which forms three binding sites for PP1 helices. Also the PP1:SDS22 interaction interface is distinct from the binding motifs of many PP1 regulators and therefore heterotrimeric complexes can be formed with other PP regulators such as PNUTS, RepoMan, inhibitor-3 and MYPT1 [76]. The holoenzyme PP1:SDS22 plays an important role in different cellular processes such as chromosome segregation, cell-shape regulation and sperm motility [76].

Sds22 regulates PP1 activity and its localization in mitosis. The complex PP1:SDS22 regulates the level of Aurora B activity at centromeres and kinetochores, which is important for successful chromosome segregation during cell division [78]. The formation of a ternary complex by binding of KLN1 to PP1:SDS22 inhibits the function of Arora B at kinetochore, while the interaction of PP1:SDS22 with Inhibitor-3 lead to PP1 inhibition, leading to the activation of Aurora B [79].

Additionally, it has been shown that PP1:SDS22 acts as tumor suppressor by inactivation of AKT and MAPK kinases, which are hyperactive in around 80% of metastatic tumors [77].

1.9 PP1 during viral infections

So far, it is known that besides HCMV also some other viruses target PP1 and affect its activity in order to ensure their propagation.

Herpes Simplex Virus 1, also a member of herpesvirus family, uses PP1 to dephosphorylate eIF2α by bridging PP1 and eIF2α. Its protein ICP34.5 contains an RVxF and an eIF2α binding motif highly similar to the human PP1 regulators targeting eIF2α [80].

Furthermore, HIV-1 transcription is regulated by PP1 [81]. The HIV-1 protein Tat (Trans-Activator of Transcription) consists of two domains, the activation domain for the interaction with host proteins and the positively charged RNA-binding domain for the interaction with HIV-1 transactivation response (TAR)

RNA [82]. Tat protein recruits the positive transcription elongation factor b (P-TEFb), containing cell cycle-dependent kinase CDK9 and cyclin T1, to the TAR RNA, leading to its transcription via the phosphorylation of RNA polymerase II (RNAPII) [81], [82]. Additionally, Tat protein regulates the dephosphorylation of CDK9 resulting in the transcriptional elongation of HIV-1 genes. Tat protein targets PP1 via a QVxF motif to dephosphorylate CDK9. The dephosphorylated CDK9 separates from 7SK RNA and the protein HEXIM1 (hexamethylene bisacetamide-inducible protein 1) which both inhibit the catalytic activity of CDK9 and in this way RNAPII CTD phosphorylation [83], [84]. It has been shown that the PP1 inhibitor 1E7-03 binds noncompetitively to PP1, without the reduction of PP1 activity, and blocks the interaction of PP1 with Tat protein, resulting repression of HIV transcription [85].

Hepatitis B virus (HBV) targets PP1 to ensure its transcription [86]. The HBV genome encodes the X regulatory protein (HBx), which interacts with PP1 and blocks its activity in order to prevent the dephosphorylation of the transcription factor CREB (cyclic adenosine monophosphate (cAMP) response element-binding protein) and thus CREB inactivation. CREB is essential for the transcription of episomal HBV genes and it is activated upon phosphorylation by cAMP [86].

Ebola virus (EBOV) also uses PP1 to regulate the phosphorylation status of the viral polymerase cofactor VP30. The phosphorylated VP30 leads to the activation of gene transcription but not genome replication. Hence, PP1 regulates the switch between viral transcription and replication [87].

Taken all together, PP1 is indeed important for viral infections and could be a potential target for drug development.

2 Aim of the thesis

Michelson et al. already showed in 1996 that the human phosphatases PP1 and PP2A are incorporated into the tegument of HCMV and that they induce a state of hypophosphorylation immediately after infection [53]. Furthermore, numerous studies have shown that PP1 is also a target for viral proteins of other viruses, including DNA and RNA viruses, contributing to their replication and spreading. Considering that PP1 is a critical regulator during virus infection, it represents an interesting topic in antiviral research as well as a potential treatment target of HCMV infection. We hypothesized that PP1 incorporation into the HCMV tegument is tightly regulated and mediated by at least one PP1-binding HCMV protein. Hence, the aim of this thesis was to investigate the potential interaction of PP1 with HCMV tegument proteins containing RVxF motifs, mainly by using a Mammalian Two-Hybrid (M2H) assay and Co-Immunoprecipitation.

Additionally, we aimed to explore the possibility that the formation of a PP1 holoenzyme with other human proteins also present in the HCMV virion allows PP1 incorporation into the viral tegument layer.

3 Materials

3.1 Reagents and buffers

Western Blot Transfer Buffer

29g glycine, 6g Tris-base and 400ml methanol dissolved in 2L. The buffer is stored at 4°C.

10xTBS

24g Tris-HCL, 5.6g Tris-base, 88NaCL are dissolved in 900ml dH_2O. The pH of the solution is 7.6 at room temperature. The pH is adjusted by addition of concentrated HCL.

Western Blot Washing buffer (TBS-T)

10xTBS diluted to 1xTBS supplemented with 0,05% Tween20.

5% Milk Blocking Buffer

5% non-fat dry milk dissolved in 1xTBS-T.

SDS Loading Dye (5X)

4% SDS, 250mM Tris, 30% glycerol, 0.05% bromophenol-blue, β-Mercaptoethanol (5%)

Polyacrylamide gels

Separating gel (8% polyacrylamide gel, final volume 5ml): 2.3ml dH2O, 1.3ml 30% Acrylamide Bis Solution, 1.3ml 1.5M Tris-HCl (pH 8.8), 50µl 10% SDS, 50µl 10% APS and 3µl TEMED were mixed.

Stacking gel (6% polyacrylamide gel, final volume 2ml): 1.4ml dH2O, 330µl 30% Acrylamide Bis Solution, 250µl 0.5M Tris-HCl (pH 6.8), 20µl 10% SDS, 20µl 10% APS and 2µl TEMED were mixed.

10x SDS-PAGE Running Buffer

30g Tris- base, 144g glycine and 10g SDS were dissolved in 1L dH_2O. The pH of the buffer is 8.3, no pH adjustment is required. 10x Running SDS Buffer was stored at room temperature and diluted to 1x before use.

Lysogeny Broth (LB) medium

LB medium was prepared by addition of 10g tryptone, 5g yeast extract and 5g NaCl in dH_2O to a final volume of 1L. This solution was autoclaved. Before use, ampicillin was added in lukewarm LB medium in a final concentration of 100µg/ml.

LB agar

15g agar-agar per liter was dissolved in LB medium of medium and autoclaved. Ampicillin was added before pouring of lukewarm LB agar in a final concentration of 100µg/ml.

ONPG solution

3mg/ml ONPG was dissolved in PBS with 100mM 2-mercaptoethanol.

3.2 Primary Antibodies

Table 1) List of primary antibodies for Western Blot and Co-IP

Antibody	Origin	Dilution	MW	Company	Product number	Purpose
PP1 alpha	mouse	1:1,000	~36kDa	Santa Cruz	sc-271762	WB
PP1(E9)	mouse	1:1,000	~36kDa	Santa Cruz	sc-7482	WB/Co-IP
GFP	rabbit	1:1,000	~27kDa	Cell Signaling Technology®	#2956	WB
CMV pp150(UL32)	mouse	1:1,000	~150kDa	Otto Majdic	non-commercial	WB
CMVpp65	mouse	1:1,000	~65kDa	Santa Cruz	sc-56976	WB/Co-IP
B-actin	rabbit	1:3,000	~45kDa	Cell Signaling Technology®	#8457	WB
B-tubulin	rabbit	1:3,000	~55kDa	Cell Signaling Technology®	#2128	WB
GAPDH	mouse	1:2,000	~37kDa	Santa Cruz	sc-47724	WB
GAPDH	rabbit	1:1,000	~37kDa	Cell Signaling Technology®	#5174	WB
6x-His Tag Antibody (HIS.H8)	mouse	1:1,000	~ 840Da	Invitrogen	#MA1-21315	WB/Co-IP
HA Tag Antibody (5B1D10)	mouse	1:1,000	~ 1.1kDa	Invitrogen	# 32-6700	WB/Co-IP

3.3 Secondary Antibodies

Table 2) List of secondary antibodies for Western Blot

Antibody	Dilution	Company	Product number
Goat Anti-Mouse IgG	1:10,000	Jackson ImmunoResearch Laboratories	115-035-008
Anti-Rabbit IgG, HRP-linked antibody	1:5,000	Cell Signaling Technology®	#7074
m-IgGk BP-HRP (anti-mouse)	1:5,000	Santa Cruz	sc-516102
Goat anti Human IgG (Fc specific) Polyclonal Antibody	1:3,000	Origene	SP1032P

3.4 Primers

Table 3) List of primers used for PCRs and colony PCRs. Melting temperature (Tm) was calculated by Thermo Fisher Scientific Tm calculator. If primers contain restriction sites (marked blue) and spacers the Tm refers only to the template-binding section. The sequences marked green correspond to His or HA tag.

Primer name	Sequence (5'-3')	Tm(°C)
SDS22-1F-cDNA	CTGCCTGTGGACATGGAAAC	59.12
SDS22-1R-cDNA	GAAGGACTCAGAACCTGACG	57.64
SDS22-2F-cDNA	GCCTGTGGACATGGAAACCA	60.54
SDS22-2R-cDNA	GCCAAGAAGGACTCAGAACC	58.19
F-EcoRI-SDS22	GGGGAATTCATGGAAACCATCAACCTGGAC	54.5
R-SDS22-BamHI	GTCGGATCCTCAGAACCTGACGAACGTGG	56.7
F-EcoRI-SDS22	GGGGAATTCATGGAAACCATCAACCTGGAC	59.9
R-SDS22-BamHI	GGTGGATCCCAGAACCTGACGAACGTGG	58.5
F1-GRB2-cDNA	CAGAAGAGGCGAGGCTAA	61.6
R2-GRB2-cDNA	TAAACCCACAAGCTGCCTCT	64.7
F2-GRB2-cDNA	GTTGCTTCAGCAGGGAAGAC	64.2
R2-GRB2-cDNA	CTGTGAGGGAGTGCAGAACA	64.8
F-EcoRI-GRB2	TAAGCAGGATCCATGGAAGCCATCGCCAAATA	68
R-GRB2-BamHI	TAATGCGGATCCAAATAGACGTTCCGGTTCACG	70.5

F-EcoRI- YWHAZ	GGGGAATTCATGGATAAAAATGAGCTGGTT	54.63
R- YWHAZ -BamHI	GGTGGATCCCAATTTTCCCCTCCTTCTCC	55.68
F- BamHI- YWHAZ	TAATGCGGATCCATGGATAAAAATGAGCTGGTT	59
R- YWHAZ-XbaI	TGCTTATCTAGATTAATTTTCCCCTCCTTCTCC	60.4
F- YWHAZ-cDNA	GAGCCAGCAGAACATCCAGT	65.3
R- YWHAZ-cDNA	TATTTGTGGGACAGCATGGA	62.4
F-EcoRI-UL24	GGG GAA TTC ATG GAG GAG ACC CGG GCG	69
R-UL24-BamHI	GGT GGA TCC CAA CGG TGC TGA CGT CCT T	66
F-EcoRI-UL82	GGG GAA TTC ATG TCT CAG GCA TCG TCC T	63
R-UL82-BamHI	GGT GGA TCC CAG ATG CGG GGT CGA CTG	65
F-UL38gDNA2	ACC AGT AAG CAG GGG TAA AC	62.6
R-UL38gDNA2	TGG TCA TCT AGC AGC AAA GT	62.3
F-KnpI_UL38	CTT GGT ACC ATG ACT ACG ACC ACG CAT A	61.3
R-UL38_XbaI	TTA TCT AGA CTA GAC CAC GAC CAC CAT CT	63.8
F-EEF1A1-cDNA	AAA AGC CAA AAT GGG AAA GG	60.4
R-EEF1A1-cDNA	CCG TTC TTC CAC CAC TGA TT	63.1
F-EEF1G-cDNA	TTT CTT TGC GGA ATC ACC AT	61.3
R-EEF1G-cDNA	TCC TTT AAT GAC CCC CAT CTC	62.3
F-EEF2-cDNA	CGA CTC GCT TCT TTC GGT TC	63.9
R-EEF2-cDNA	AAG TGT TGG GTG TCC CAT CC	65.3
F_NheI_EEF1G	AAG CTG GCT AGC ATG GCG GCT GGG ACC CT	69.2
R_EEF1G_BsiW	GAC GTA CGT CAC TTG AAG ATC TTG CCC TGA	64.6
F_EcoRI_EEF1A1	GGG GAA TTC ATG GGA AAG GAA AAG ACT C	57.8
R_EEF1A1_BamHI	GGT GGA TCC CAT TTA GCC TTC TGA GCT T	58.3
F_BamHI_EEF1A1	CTC GGA TCC ATG GGA AAG GAA AAG ACT C	57.8
R_EEF1A1_XbaI	CCC TCT AGA TCA TTT AGC CTT CTG AGC TT	59.9
F_EcoRI_EEF2	GGG GAA TTC ATG GTG AAC TTC ACG GTA GA	61.7
R_EEF2_BamHI	GGT GGA TCC CAC AAT TTG TCC AGG AAG TT	59.4
F_BamHI_EEF2	CTC GGA TCC ATG GTG AAC TTC ACG GTA GA	61.7
R_EEF2_XbaI	CCC TCT AGA CTA CAA TTT GTC CAG GAA GTT	59.1
F-His-PP1	ATGGATCCATGCACCACCACCACCACCACTCCGACAGCAGAAGCTC	64.3

F-HA-SDS22	ATGAATTCATGTACCCATACGATGTTCCAGATTACGCTGAAAC-CATCAACCTGGACAG	61.6
F-BamHI-PP1CA	ACG GGA TCC ATG TCC GAC AGC GAG AAG	62.1
R- PP1CA-XbaI	TGC TCT AGA CTA TTT CTT GGC TTT GGC GG	62.5

3.5 Sequencing Primers

Table 4) List of primers used for the sequencing of plasmids

Primer name	Sequence
F-pM-Gal4	GAGTAGTAACAAAGGTCAAA
R-pM-GFP	GTCTTGTAGTTGCCGTCGTC
R-pM	ATTTTATGTTTCAGGTTCAGG
F-UL32-RVXF-seq	GTCGGTGTTCCTTCCTTGAA
R-pcDNA	AGGGAAGAAAGCGAAAGGAG
F-CMV-prom	CGCAAATGGGCGGTAGGCGTG

3.6 Primers for Site-Directed Mutagenesis

Table 5) Primers used to introduce a mutation in the RVxF motif of UL32 in pcDNA

Primer name	Sequence	Tm(°C)
F-UL32 $_{KTAAA}$	CGGGCATGAAAACGGCCGCTGCCGACCTATCGTCGCCC	84.1
R-UL32$_{KTAAA}$	CGATAGGTCGGCAGCGGCCGTTTTCATGCCCGTCG	81.4

3.7 Plasmids

Table 6) Plasmids used in this study

Plasmid	Purpose	Source
pM	M2H	Berger group, Center for Brain Research (CBR), University of Vienna
pVP16	M2H	Berger group, Center for Brain Research (CBR), University of Vienna

pVP16AD/Gal4BD	M2H	Berger group, Center for Brain Research (CBR), University of Vienna
pCMV-Gal	M2H	Berger group, Center for Brain Research (CBR), University of Vienna
pFR-Luc	M2H	Berger group, Center for Brain Research (CBR), University of Vienna
pM-GADD34$_{(553-568)}$-GFP	M2H	Steininger group, Cloned by Ana Katic
pM-UL32$_{(997-1012)\ WT}$-GFP	M2H	Steininger group, Cloned by Ana Katic
pM-UL32$_{(997-1012)\ KTAAA}$-GFP	M2H	This study
pM-UL32$_{(437-1048)\ C\text{-}terminus}$	M2H	Steininger group, Cloned by Ana Katic
pcDNA-UL32$_{WT}$	Co-IP	Steininger group, Cloned by Ana Katic
pcDNA-UL32$_{KTAAA}$	WB	This study
pM-UL32$_{WT}$	M2H	Steininger group, Cloned by Ana Katic
pM-SDS22	M2H	This study
pM-SDS22-GFP	M2H/Co-IP	This study
pM-HA-SDS22	Co-IP	This study
pM-GRB2-GFP	M2H/Co-IP	This study
pM- YWHAZ (14-3-3)-GFP	M2H	This study
pcDNA-YWHAZ	Co-IP	This study
pcDNA-PP1α	Co-IP	This study
pcDNA-HIS-PP1	Co-IP	This study
pcDNA-pp65	M2H/Co-IP	Steininger group, Cloned by Franz Rieder
pM-UL24-GFP	M2H	This study
pM-UL38	M2H	This study
pM-UL82-GFP	M2H	This study
pcDNA-EEF2	Co-IP	This study
pM-EEF2-GFP	M2H	This study
pcDNA-EEF1A1	Co-IP	This study

pM-EEF1A1-GFP	M2H	This study
pcDNA-EEF1G	Co-IP	This study
pcDNA3.1-hygro-lacZ	Cloning	Thermo Fisher Scientific

3.8 Oligonucleotides

Table 7) Mutated UL32 Oligonucleotides for the cloning into pM-GFP vector (EcoRI/BamHI). The complementary oligonucleotides consist of simulated digested restriction sites, marked by bold letters and a mutated RVxF motif, marked by red letters. The indicated amino acids represent the peptide position within the full-length protein.

Protein	Amino acids	Sequence
UL32	997-1012	5' **AATT**CACGGGCATGAAAACGGCTGCTGCTGACCTATCGTCGCCCCAGAAGAGCGGTGG**G** 3' **GATCC**CCACCGCTCTTCTGGGGCGACGATAGGTCAGCAGCAGCCGTTTTCATGCCCGT**G**

4 Methods

4.1 High fidelity polymerase chain reaction (iProof™polymerase)

The PCR reaction mix contained 10µl 5x iProof HF buffer, 0.5µl iProof DNA polymerase, each 2.5µl of 10µM forward and reverse primer, 1µl 10mM dNTP mix, 1.5µl DMSO, 1.5µl MgCl2 and as DNA template, 10ng of pure DNA plasmid or 400ng cDNA in a final volume of 50µl. The PCR program contained the following steps: initial denaturation was at 98°C for 30s, next cycles of 98°C for 10s and annealing for 20s at the temperature corresponding to the melting temperature of primers used. Elongation was performed at 72°C for 30s per 1kb of PCR product. The cycle was repeated 30 to 35 times. Final elongation was at 72°C for 10min, afterwards samples were held at 4°C.

4.2 Standard polymerase chain reaction (iTaq™ polymerase)

The PCR reaction mix contained 5µl iTaq buffer (10x), 2.5µl of each 10µM forward and reverse primer, 1.5µl MgCl2, 1µl 10mM dNTP mix, 0.25µl iTaq™DNA polymerase and DNA template, 10ng of pure DNA plasmid or 400ng cDNA in a final volume 50µl. Initial denaturation was set at 95°C for 3 minutes. Next denaturation was performed at 95°C for 30 seconds, annealing for 30 seconds at the respective primer melting temperature and elongation was at 72°C for 1min per 1kb of PCR product. The cycles were repeated 30 to 35 times. The PCR products were held at 4°C.

4.3 Colony PCR

Colony PCR was performed according to the protocol for iTaq™DNA polymerase as described above. As DNA template for colony PCR bacterial colonies were used, which were inoculated in 10µl dH_2O.

4.4 Gel electrophoresis

PCR products, mixed with Orange G, were analysed on 1% agarose gels, which were prepared with agarose and 1x TAE buffer. A 100bp or 1kb DNA ladder was used as a reference. Gels were run at 80V – 120V.

4.5 Restriction Digest

1µg plasmid DNA or PCR product was digested with 1µl of each Fast Digest restriction enzyme (Thermofisher) in 1x FastDigest Buffer at 37°C for 30 minutes. The digestion was inactivated at 80°C for 5min. The fragments were separated by gel electrophoresis and purified with the QIAquick Gel

Extraction Kit (Qiagen). EcoRI and BamHI were used for cloning insterts into the pM vector, while BamHI and XbaI were used for cloning of inserts into pcDNA.

4.6 Ligation

The ligation mix contained 100ng backbone, varying amounts of insert, 0.6µl T4 DNA ligase (company), 2µl 1x T4 ligation buffer and nuclease free H_2O in a final volume of 20µl. A vector/insert ratio of 1:4 was used for ligation. The amount of insert to be used was determined by using the following formula:

$$\frac{ng\ of\ vector \times kb\ size\ of insert}{kb\ size\ of\ vector} \times \frac{molar\ ratio\ of insert}{vector}$$

4.7 Transformation of *E. coli* DH5α

40µl of DH5α competent cells were added to the DNA sample (either a ligation mix or 100ng plasmid DNA), mixed gently without pipetting up and down and the mix was incubated at 4°C for 30 minutes. Afterwards, the transformed bacteria were exposed to a heat shock at 42°C for 30 seconds. Next, 250µl of S.O.C. medium was added and transformed bacteria were incubated at 37°C for 60 minutes while shaking. Next, transformed bacteria were spread on an LB-Amp agar plates and incubated at 37°C overnight.

4.8 Glycerol Stocks

Bacterial overnight cultures were mixed with 50% glycerol (diluted with dH_2O) in the ratio of 1:2 and the samples were stored at -80°C. For recultivation, a small piece of frozen glycerol sample was added with a pipette tip into LB medium containing ampicillin.

4.9 Plasmid purification

After transformation, plasmids were isolated by using QIAprep Spin Miniprep (Qiagen) Kits following the manufacturer's instructions and eluted with elution buffer. For transfection of mammalian cells, plasmids were purified with the Qiagen Plasmid Midi Kit, where the precipitated DNA pellets were dissolved in dH_2O. The samples were stored at -20°C.

4.10 DNA sequencing

Sanger Sequencing was performed by Microsynth AG. 1200ng of purified plasmid was diluted with dH_2O to the final volume of 12µl and mixed with 3µl of 10µM primer.

4.11 RNA isolation

In order to isolate RNA, the PureLink™ RNA Mini Kit (Invitrogen) was used. Surfaces and pipettes were wiped down with RNaseZap™ (Invitrogen). During the purification process, gloves were frequently changed and samples were kept on ice the whole time. HeLa cells grown in 75cm^2 flasks (Cellstar) were trypsinized and approximately 8x10^6 were used for RNA isolation. First, cells were transferred to a 15ml tube and pelleted at 300xg for 5 min. Next, the cells were washed with 1ml of cold 1x PBS. After removal of PBS, 300µl of cold lysis buffer (supplemented with 1% 2-mercaptoethanol) was added and cells were detached by pipetting up and down. The cell suspension was transferred to a fresh tube and centrifuged for 2min at 12000g. One volume of 70% ethanol (100% molecular grade ethanol diluted with ddH2O) was added to one volume of cell lysate (=300µl) and mixed by pipetting up and down. This mixture was transferred to a spin column inserted in a collection tube and spinned for 15s at 12000g. The flow-through was discarded and the column was reinserted into the collection tube. 700µl of Wash Buffer I were added to the column and centrifuged for 15s at 12000g. The flow-through was discarded and the column was reinserted into a new collection tube. 500µl of Wash Buffer II were added to the column and centrifuged for 15s at 12000g. The flow-through was discarded and this step was repeated, with an incubation of Wash Buffer II for 1min after addition to the column. Then, column and collection tube were spinned empty for 1min at 12000g to remove remaining buffers. The column was inserted into an elution tube and 40µl of pre-heated RNase-free water (55°C) were added directly onto the membrane and incubated for 1min followed by centrifugation for 1min at 12000g. RNA concentration was measured on a NanoDrop 8000 instrument. RNA sample was stored at -80°C.

4.12 cDNA synthesis

Immediately after RNA isolation, cDNA was synthesized using the iScript™ cDNA Synthesis Kit (BioRad). In PCR tubes, 1µg RNA, 4µl 5x iScript reaction buffer, 1µl iScript reverse transcriptase and RNase free water were mixed adding up to a total volume of 20µl. The PCR program contained the following steps: 25°C for 5min, 46°C for 20min and 96°C for 1min. cDNA samples were stored at -20°C.

4.13 Cell culture

HeLa and HEK293 cells were grown in DMEM medium (Gibco) containing 10% FBS and 1x Antibiotic-Antimycotic mix (penicillin and streptomycin) at 37°C, 5% CO2. Every 2-3 days, the cells were trypsinized and subcultured in a ratio of 1:10 or 1:2.

For long-term storage, cells were pelleted (300-500g, 5 min), washed with 1x DPBS, pelleted again and resuspended in 1ml cultivation medium and 100µl DMSO. Then cells were frozen at -80°C for 3-7 days and afterwards transferred to liquid nitrogen.

For recultivation, frozen cells were thawed in a water bath (ca. 37°C) and immediately diluted with 10ml cultivation medium. Then, cells were centrifuged (500g, 5 min.), washed with 1x DPBS, centrifuged again and resuspended in cultivation medium. The cells were cultured as described above.

4.14 Cloning of Mammalian Two-Hybrid Assay Vectors

4.14.1 Mammalian Two-Hybrid Assay Vectors

The human proteins were amplified from cDNA from human foreskin fibroblasts (HFF) or HeLa cells (see 4.12), while HCMV tegument proteins from DNA of HCMV, by PCR with iProof™High Fidelity DNA polymerase. Next, PCR addition of restriction sites was performed (used primers see Table 3). Afterwards, the fragments and pM-GADD34-eGFP were cut by EcoRI and BamHI. The cut fragments and the linearized vector were analyzed by gel electrophoresis and subsequently purified with the QIAquick PCR purification Kit and QIAquick Gel Extraction Kit. Finally, the inserts were ligated (see 4.6) with digested pM-eGFP and amplified by transformation of *E. coli* DH5α. After transformation of *E. coli* DH5α and plasmid purification via miniprep, the correct sequence of the insert was verified by colony PCR and sequencing.

4.14.2 Annealing of oligonucleotides for cloning

A UL32 peptide construct containing a mutated RVxF motif was created by annealing of DNA oligonucleotides with overhanging ends (see Table 7). Annealing was performed with 5µl of each 10µM oligonucleotide stocks, 2.5µl 10x T4 ligation buffer and 12.5µl dH2O. Then, the prepared sample was incubated on a Thermocycler with the following program: 95°C for 2 minutes, 95°C for 30 seconds, cooling down to 12°C while reducing the temperature for -1°C/30 sec and storage at 12°C.

4.14.3 Insertion of peptide sequence into pM vector

After annealing of oligonucleotides, these fragments were inserted in frame into the pM-eGFP vector, creating a construct that is a fusion of Gal4-DNA binding domain, the peptide and GFP that allows live monitoring of its expression in cells via detection of the fluorescent signal. For ligation of oligonucleotides containing EcoRI and BamHI restriction sites, 2µl of the annealed oligonucleotide and

100ng of EcoRI/BamHI digested pM were mixed. The sequence of the inserted fragments was verified by DNA sequencing.

4.15 Mammalian Two-Hybrid Assays

4.15.1 Transfection of HeLa cells

For M2H assays, HeLa cells were seeded in 24 well plates. 10^5 cells were seeded with 1ml cultivation medium 24h before transfection to ensure 70-80% confluency at the time point of transfection. Transfections were performed according to the instructions provided with the TurboFect™Transfection Reagent (Thermofisher Scientific). Each well was transfected with 2µl TurboFect™Transfection Reagent and with a total of 850ng plasmid DNA, consisting of 50ng pCMV-Gal, 100ng pFR-Luc and each 350ng bait and prey plasmid. Transfected cells were incubated for 48h at 37°C, 5% CO_2.

4.15.2 Fluorescence microscopy

In order to check the expression of proteins or peptides, fluorescence microscopy was used for detection of GFP signal 24h after transfection.

4.15.3 Harvesting of HeLa cells

Cells were harvested on ice 48h after transfection. The cells were washed by using cold DPBS and lysed with 100µl 1x Cell Culture Lysis Reagent (Luciferase Cell Culture Lysis 5x Reagent, Promega, diluted in dH_2O and supplemented with 1% Halt Protease/Phosphatase inhibitor) per well. Next, the lysates were centrifuged at 13.000rpm at 4°C for 20 minutes. The supernatants were transferred into new tubes and used for the measurements. The samples were stored at -20°C until Western blot analysis.

4.15.4 Measurement of luciferase activity

For measurement of luciferase activity, 10µl of cell lysate was loaded into a 96 well plate with black walls and white bottom. 50µl luciferase assay reagent (Promega) was dispensed into each well on a Varioskan™ LUX multimode microplate reader (Thermo Fisher Scientific) and luminescence signal was measured for 1 and 10 seconds immediately after dispensing.

4.15.5 Measurement of β-galactosidase activity

β-galactosidase activity was measured in 96 well plates. 10µl of cell lysate and 100µl of ONPG solution were loaded per well. The plate was incubated at 37°C until the samples developed a yellow color. Absorbance was measured in a microplate reader at a wavelength of 420nm.

4.15.6 Normalization and Analysis of M2H assay

For analysis of the M2H assay, luminescence values were normalized to β-galactosidase activity in order to compensate differences caused by unequal transfection efficiency, different cell numbers, as well as differences in gene expression rates. In order to compare independent assays, the results were normalized to the values obtained for the positive control, pVP16AD/Gal4BD. VP16 AD is fused to the DBD, which leads to constitutive activity of pVP16AD/Gal4BD, providing the maximum transcription of luciferase in the cells. All data obtained by M2H assays were analyzed using GraphPad Prism 6.

4.16 Co-Immunoprecipitation (Co-IP)

4.16.1 Co-IP vectors

Co-IP was to use to identify protein-protein interactions by using target protein-specific antibodies to indirectly capture proteins that are bound to a specific target protein, PP1. For used plasmids see Table 6. The principle of vector cloning was the same as for M2H vectors (see 3.14.1.).

4.16.2 Transfection of HeLa cells

In order to perform Co-IP, $2.2x10^6$HeLa cells were seeded in 10cm cell plates with 10ml cultivation medium. According to the instructions provided with the TurboFect™Transfection Reagent, transfection was performed approximately 24h after seeding. The cells were transfected with a total of 10µg plasmid DNA, consisting of 4µg pcDNA-PP1α and 6µg potential PP1 binders. Afterwards, the cells were incubated for 48h at 37°C, 5% CO_2.

4.16.3 Harvesting of HeLa cells

The cells were washed with cold DPBS on ice and harvested with 500µl Lysis buffer containing 50mM Tris, 500mM NaCl, 1% NP40, 0.1% SDS and 1% “Halt” protease and phosphatase inhibitor (Thermofisher Scientific). The cells were incubated for 5min in lysis buffer. After incubation, the cell layer was scraped off with a pre-chilled scraper and transferred into new tubes. Then, the cell lysates were centrifuged for 15min at 10,000g at 4°C. The pellets were removed and the supernatants were used for measurement of protein concentration. Sample protein concentrations were measured with the Pierce™BCA Protein Assay Kit according to the manufacturer’s manual.

4.16.4 Co-Immunoprecipitation

For Co-IP, 500µg protein was mixed with 1xTBS up to a total volume of 1ml. In order to pre-clean the lysate, 20µl of Protein A/G plus agarose (Santa Cruz Biotechnology) were added to the sample and incubated at 4°C for 30min. After incubation, the sample was centrifuged for 5min at 2500rpm at 4°C.

The supernatant was transferred to a new tube and incubated with 2µg primary antibody (see Table 1) for 1h at 4°C. In the next step, 20µl of Protein A/G plus agarose was added to the sample and incubated at 4°C on a rotating device overnight. The immunoprecipitates were collected by centrifugation at 2500rpm at 4°C for 1min. After centrifugation, the supernatant was saved and stored at -20°C for analysis by western blot, while the pellet was washed four times by 1ml DPBS, each time repeating the centrifugation step above. After the first wash, the supernatant was saved and stored at -20°C for further analysis. In the final step, the pellet was resuspended in 30µl 2x Loading Dye (5x Loading Dye diluted in dH_2O), boiled at 70°C for 10min and stored at -20°C.

4.17 Site-Directed Mutagenesis by PCR amplification

A point mutation in the RVxF domain of UL32 in pcDNA-UL32 was introduced by site-directed mutagenesis via PCR. To introduce a mutation in a vector, both of the primers should contain the targeted mutation. According to the protocol of Tom Richard (Penn State University), the mutation can be as close as 4 bases from the 5-terminus and at least 8 bases from the 3-terminus. At the 3-terminus of both primers should be introduced at least eight non-overlapping bases. At least one C or G should occur at the end of each primer and the melting temperature should be greater than 78°C. After designing primers matching these specifications (see Table 5), PCR with iProof™ High Fidelity DNA polymerase was performed to amplify the entire plasmid template (pcDNA-UL32, produced in DH5a *E. coli*). Then, the PCR product was incubated with the methylation-dependent endonuclease DpnI for 3h at room temperature in order to remove the parent template. DpnI was inactivated by incubation at 80°C for 5min. Next, the PCR product was purified using the QIAquick Gel Extraction Kit. After transformation of *E. coli* DH5α and plasmid purification via miniprep, the inserted mutation was verified by colony PCR and sequencing.

4.18 SDS-PAGE

After determination of protein concentration, cell lysates were mixed with 20% 5X Loading Dye for SDS-PAGE. The samples "input" of Co-IP were loaded with the amount of 25µg per well. In order to reduce and denature the samples, they were boiled at 95°C for 5min. Mini-Protean TGX gels (precast 4-15% gradient gels, Bio-Rad) for Co-IP or 8% self-made acrylamide gels for M2H samples (see the recipe above) were mounted into a Mini Trans-Blot Cell (Bio-Rad) filled with 1x SDS-running buffer. The prepared samples and 7µl of the PageRuler™ Plus Prestained Protein Ladder 10 to 250 kDa (Thermo Fisher Scientific) for the determination of protein size were loaded onto the gels. SDS-PAGE was performed at 80V for ~20min followed by 100V until loading dye front reached the bottom of the gel.

After SDS-PAGE, gels were stored in a tray containing ddH2O followed by immediate wet transfer (see below).

4.19 Western Blot Analysis

The proteins from the gel were transferred to a PVDF membrane (Thermo Scientific™), pre-activated for a few seconds in 100% methanol. The blotting was performed in 1xTransfer buffer at 4°C for 1h at 100V. An ice block in the blotting tank and constant stirring was applied to avoid local overheating. Transfer of proteins to the membrane was checked by using Ponceau S staining. Then, membranes were incubated for 1h in either Starting blocking buffer (StrartingBlock™ TBS Blocking buffer, Thermo Scientific™) or 5% milk blocking buffer. Membranes were incubated with primary antibody or human serum at 4°C overnight, then with secondary antibody at room temperature for 1h. Proteins were detected with SuperSignal West Pico PLUS Chemiluminescent Substrate or SuperSignal West Femto Maximum Sensitivity Substrate in a ChemiDoc™Imaging System. In the case of detection of two different proteins with similar molecular weight, the membrane was incubated with stripping buffer (Restore™ PLUS Western Blot Stripping Buffer, Thermo Scientific™) for 10-15min at room temperature and then reprobed. Between all steps, the membrane was washed three times for 5min with 1xTBS 0.05% Tween.

5 Results

5.1 Validation of the interaction between PP1α and UL32

5.1.1 Interaction of PP1α and the UL32$_{(997\text{-}1012)\ KTAAA}$ oligonucleotide

The second most abundant HCMV tegument protein, UL32 comprises four RVxF motifs and a SILK motif which might mediate PP1 binding. Previous experiments in our lab investigated the PP1α binding potential to the four RVxF motifs found in UL32 by M2H. For this purpose, RVxF-containing peptides in a length of 16 amino acids were created and cloned into the pM-GFP fusion protein bait vector. The results have shown that of four UL32 peptides, the peptides UL32$_{64\text{-}77}$ and UL32$_{997\text{-}1012}$ induce luminescence signals upon interaction with PP1α similar to RVXF-containing peptides from known PP1 binders [88]. In order to show specificity of RVXF-mediated binding of UL32 fragments to PP1, we subcloned a mutated UL32 fragment into a pM-GFP fusion vector (pM-UL32$_{(997\text{-}1012)\ KTAAA}$-GFP). Beside UL32 peptides, we also included the peptide GADD34$_{553\text{-}568}$, which comprises an RVxF as well as a ϕϕ motif. The GADD34$_{553\text{-}568}$ was shown to be a robust PP1 binder in previous research of our group and in this assay it was used as a positive control.

Our results show that the luminescence signals induced by UL32$_{(997\text{-}1012)\ WT}$ and UL32$_{(997\text{-}1012)\ KTAAA}$ are low and comparable to each other, indicating that the integrity of the RVxF motif is not necessary for the signal induced by the interaction with PP1. Compared to the positive control GADD34$_{553\text{-}568}$, UL32$_{(997\text{-}1012)\ WT}$ and UL32$_{(997\text{-}1012)\ KTAAA}$ provided less signal (**Figure 2**).

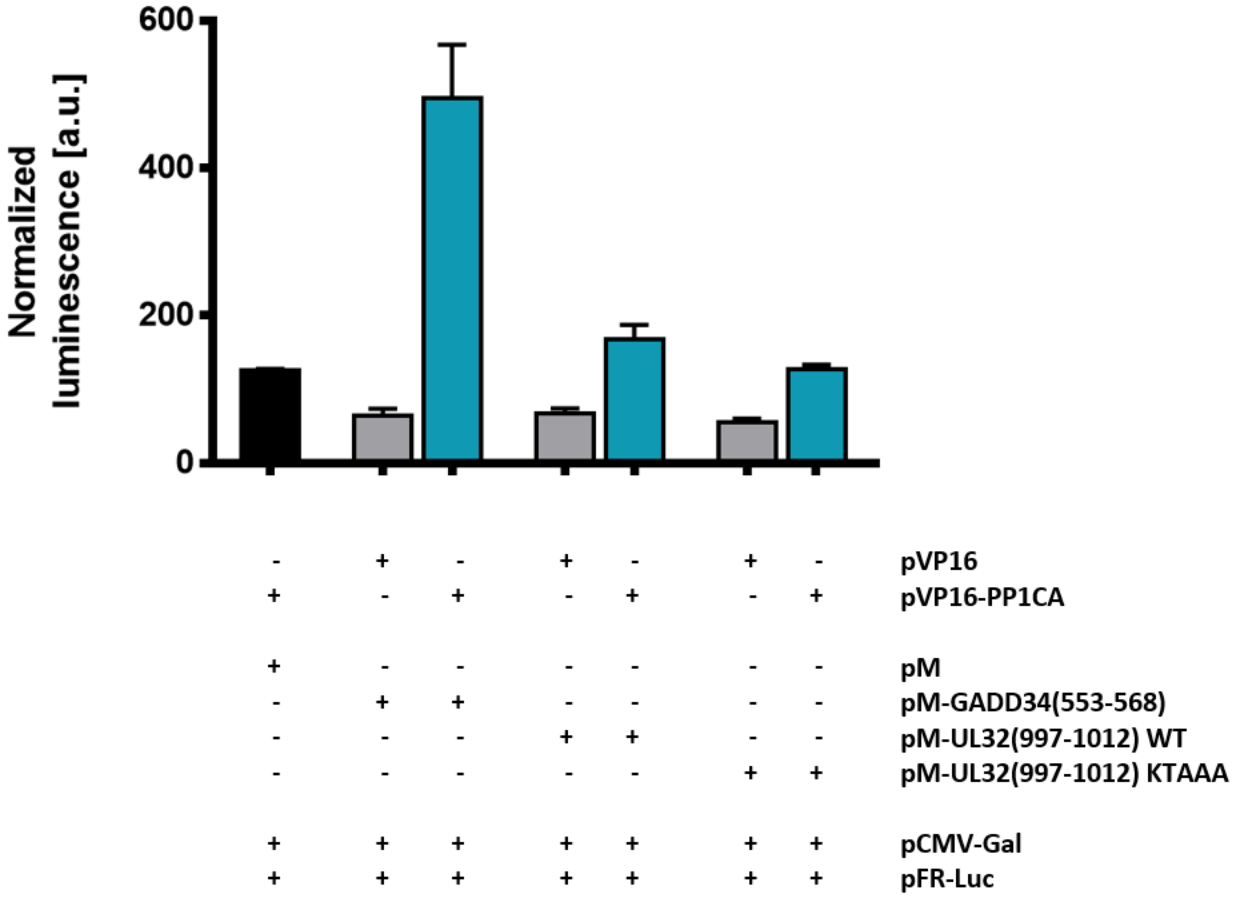

Figure 2) Interaction between UL32 peptides and PP1α. The peptides UL23(997-1012) WT and UL23(997-1012) KTAAA were tested for PP1 binding activity in an M2H assay. HeLa cells were transfected with the listed plasmids. pM-GADD34 (553-568) represents positive control. The numbers in brackets indicate the first amino acid of the peptide. Luciferase and β-galactosidase activities were measured 48h post transfection. The bars show luminescence normalized against β-galactosidase expression as a marker of transfection efficiency (mean ± SEM from technical triplicates). n=1.

Before harvesting cellular lysates for the M2H assay, the GFP expression of GFP-fused peptides transfected in the cells was verified by using fluorescence microscopy. The results show, that GFP was expressed in all samples (**Figure 3**).

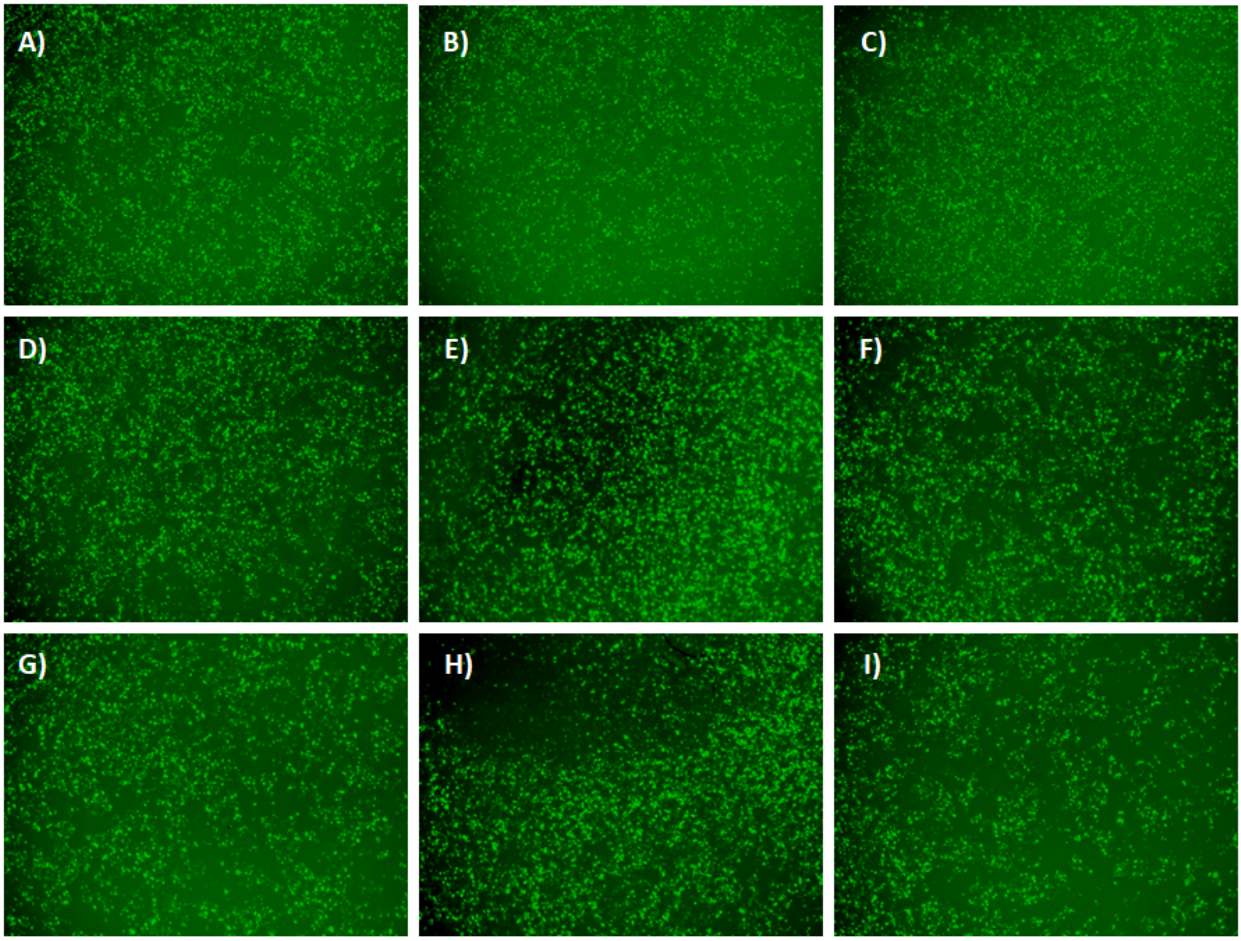

Figure 3) Detection of GFP expression in HeLa cells. HeLa cells were transfected for M2H assay with pM-GADD34(553-568)-GFP (A, B, C), UL23(997-1012)-GFP WT (D, E, F) and UL23(997-1012)-GFP KTAAA (G, H, I). GFP expression was observed by fluorescence microscopy 48 hours after transfection. Images were taken using auto exposure.

In order to ensure that low luciferase expression is not caused by low transfection efficiency or impaired expression of transfected plasmids, we additionally detected the expression of PP1 and GFP by Western Blot. The same cell lysates of transfected HeLa cells for which M2H-based luminescence was measured were used for Western Blot. We noticed that the VP16AD-PP1α fusion protein was expressed in all samples and it was clearly distinguishable from endogenous PP1 which is approximately 30kDa smaller. GFP was expressed in different amounts, while in some samples it was hardly detected despite earlier detection by immunofluorescence microscopy (**Figure 4**).

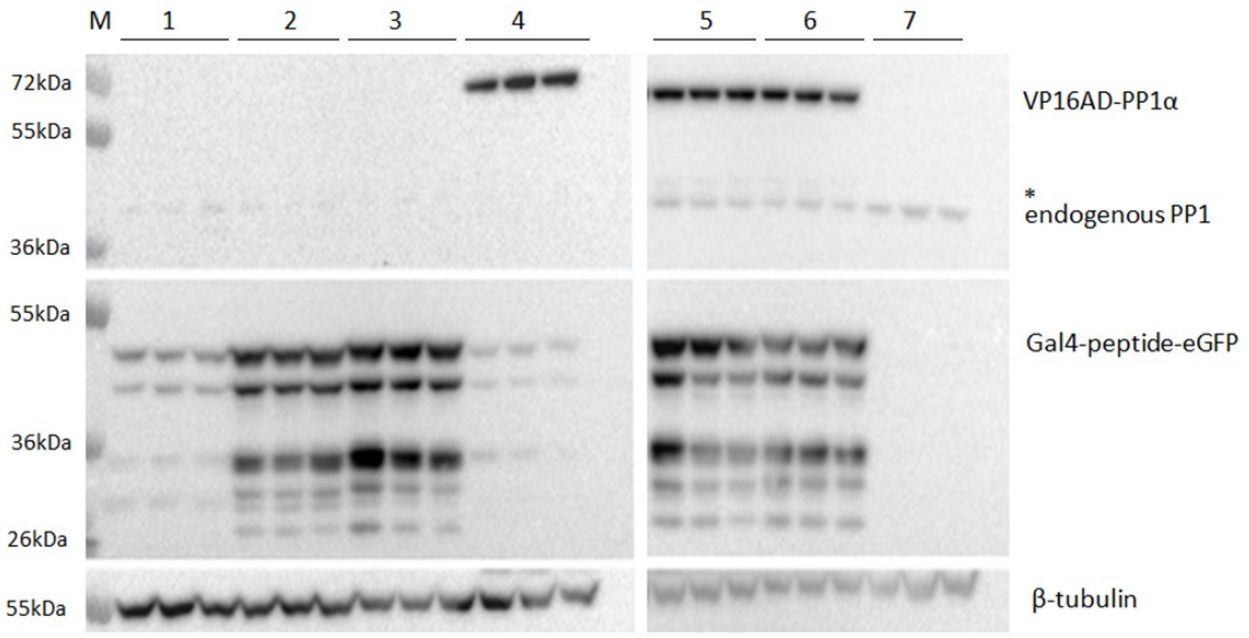

Figure 4) Detection of VP16AD-PP1 and Gal4BD-peptide-eGFP fusion proteins in lysates of transfected HeLa cells. HeLa cells were transfected for the M2H assay with pVP16 and pM-GADD34(553-568)-GFP (1), pVP16 and UL32(997-1012)-GFP (2), pVP16 and UL32(997-1012) KTAAA-GFP (3), pVP16-PP1CA and pM-GADD34(553-568)-GFP (4), pVP16-PP1CA and UL32(997-1012)-GFP (5), pVP16-PP1CA and UL32(997-1012) KTAAA-GFP (6). Untransfected cells were loaded as a negative control (7). PP1, GFP and GAPDH were detected using the respective monoclonal antibodies and HRP-linked secondary antibodies. M = marker, PageRuler Plus Prestained Protein Ladder. * indicate off-target bands.

5.1.2 Expression of mutated UL32 in HEK293 cells

To further investigate UL32 as a potential PP1 binder, our aim was to perform an M2H assay with wild-type, full-length UL32. We also generated a UL32 variant with a mutated "RVxF" motif ($UL32_{KTAAA}$) using PCR-based site directed mutagenesis (**Figure 5**). The created plasmids were transfected into HEK293 cells and the level of $UL32_{KTAAA}$ expression was checked 48h after transfection by Western Blot.

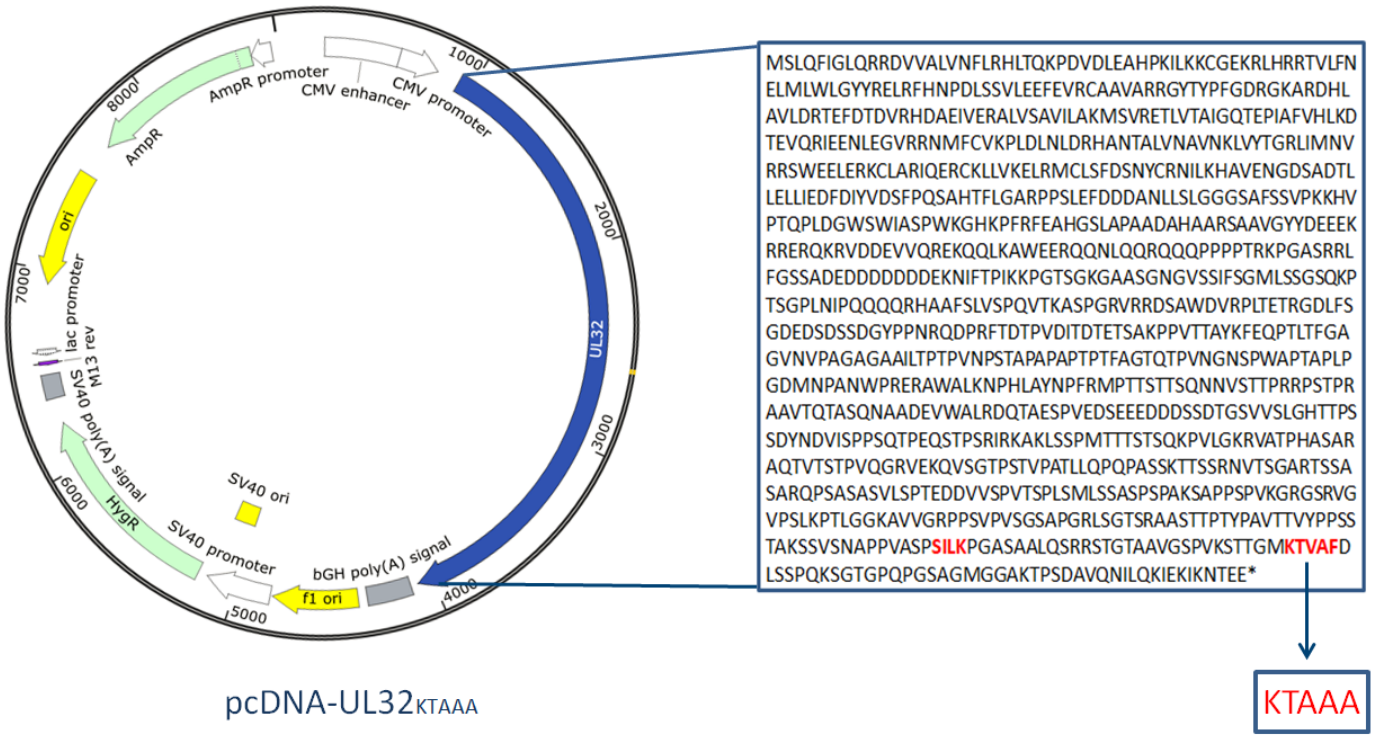

Figure 5) $UL32_{KTAAA}$ plasmid map. Mutation of KTVAF motif at the C terminus of UL32 into KTAAA using PCR-based site directed mutagenesis.

Our results show similar expression of $UL32_{WT}$ and $UL32_{KTAAA}$ in transfected cells (**Figure 6**). Also, the mutation did not prevent binding of the monoclonal α-UL32 antibody to the protein.

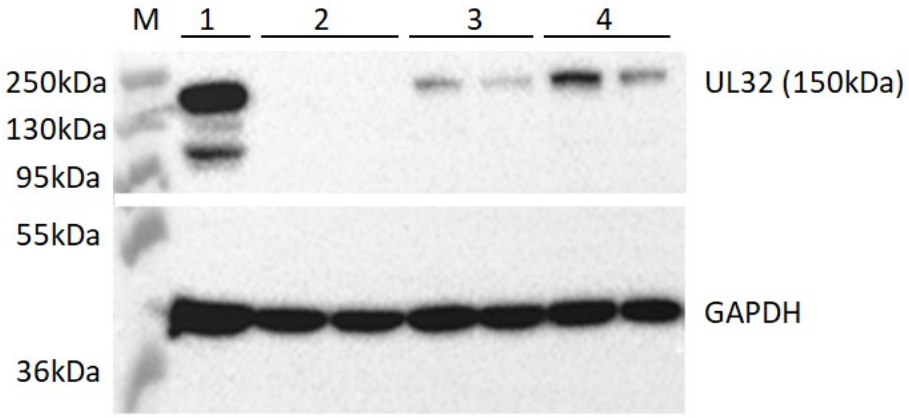

Figure 6) The expression levels of full length $UL32_{KTAAA}$ and $UL32_{WT}$ in lysates of transfected HEK293 cells. HEK293 cells were transfected with UL32WT (3) or UL32KTAAA (4). Untransfected cell lysates were

loaded as a control (2). The cells were harvested and lysed 48h after transfection. The expression levels of proteins were analyzed after Western Blotting and antibody staining. The expression levels of UL32WT and UL32KTAAA were compared to the level of UL32 from HCMV infected HFF lysate (1). M = marker, PageRuler Plus Prestained Protein Ladder.

5.1.3 Interaction of PP1α with full-length UL32

In order to validate a potential protein-protein interaction with full-length UL32, we performed two M2H assays comparing it to the peptide-based system used so far, or full-length SDS22, a well-known PP1 regulator. After measurement of the luminescence signal we could see a strong signal for the newly established positive control of SDS22-PP1α interaction (**Figure 7B**). Additionally, the peptide GADD34 induced luciferase expression less efficiently than SDS22 upon interaction with PP1α. In contrast to the positive control as well as to the peptide GADD34, no interaction occurred between PP1α and UL32 (**Figure 7A-B).** In this assay, we also tested the interaction of C-terminal fragments of $UL32_{437-1048}$ and PP1. In the comparison to $GADD34_{553-568}$, we were not able to observe any luciferase activity upon co-transfection of PP1 and $UL32_{437-1048}$ (**Figure 7A**).

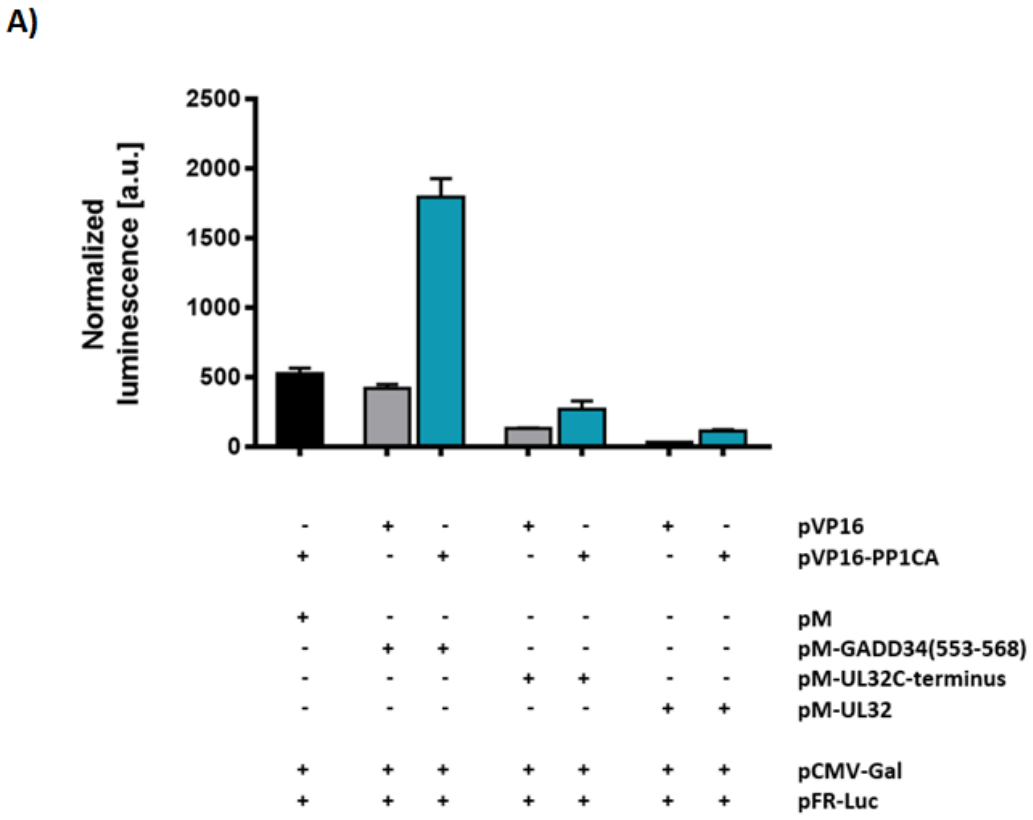

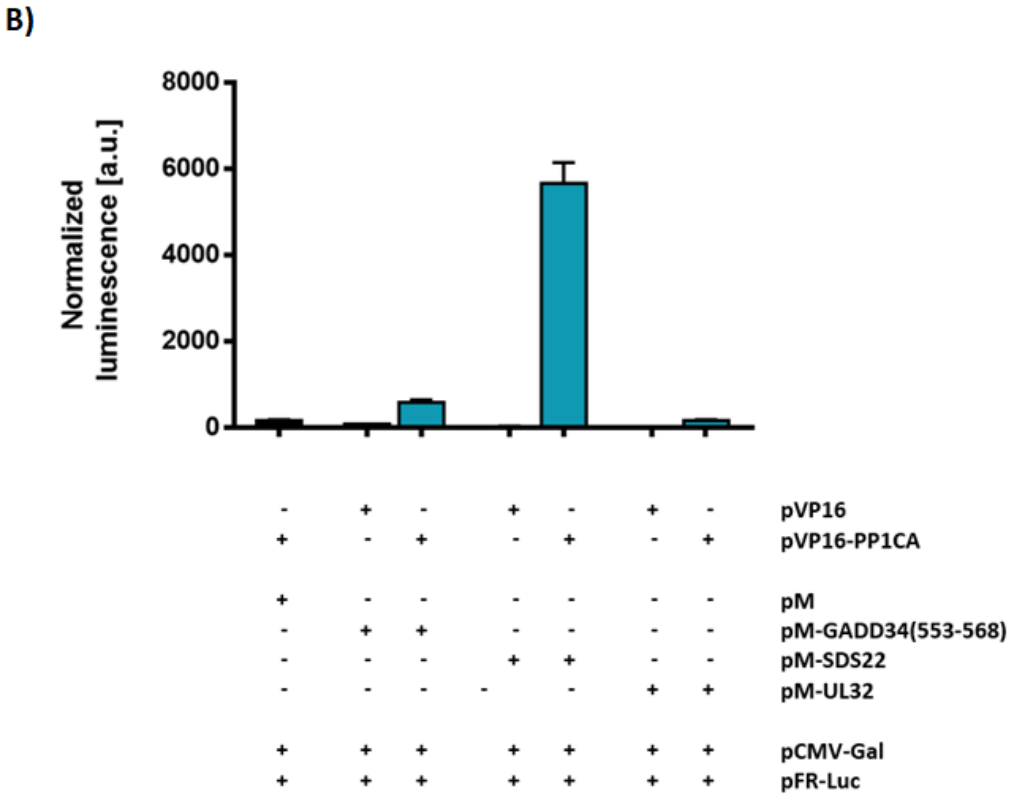

Figure 7) Interaction of full length UL32 and UL32 C-terminus fragment with PP1α. The full length UL32 (A, B) and UL32C-terminus (A) were tested for their PP1 binding potential in M2H assays. HeLa cells were transfected with the listed plasmids. pM-GADD34 (553-568) and pM-SDS22 represent positive control. The numbers in brackets indicate the first amino acid of the peptide within the protein. Luciferase and β-galactosidase activities were measured 48h post transfection. The bars show luminescence normalized against β-galactosidase expression as a marker of transfection efficiency (mean ± SEM from technical triplicates). n=1.

In order to check whether UL32 and $UL32_{437-1048}$ are expressed in the cells, we performed Western Blot by using the lysates of HeLa cells transfected for the M2H assay. Our results show weak bands for UL32 and $UL32_{437-1048}$ compared to HCMV-infected fibroblasts used as a positive control, indicating a low level of their expression in the cells. Also, we could observe the presence of smaller bands in the $UL32_{437-1048}$ lysates, suggesting a possible degradation of the protein (**Figure 8**).

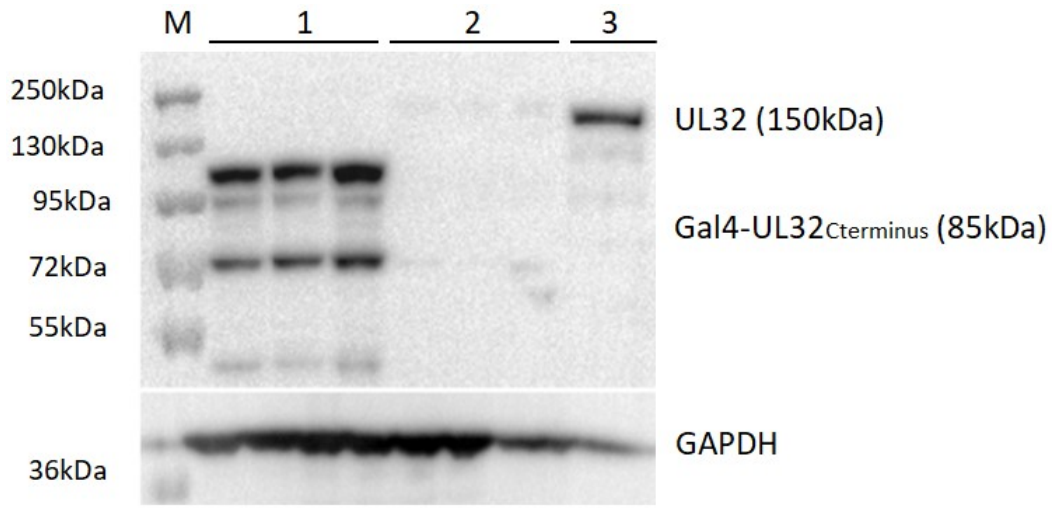

Figure 8) Detection of $UL32_{C\text{-}terminus}$ and $UL32_{WT}$ in lysates of transfected HeLa cells. For the M2H assay, HeLa cells were transfected in triplicate with pVP16-PP1CA and pM-UL32C-terminus (1) or pVP16-PP1CA and pM-UL32WT (2). The expression levels of UL32C-terminus and UL32WT were compared to the level of UL32 form HCMV infected HFF lysate (3). M = marker, PageRuler Plus Prestained Protein Ladder.

5.2 The interaction of PP1 and RVxF-containing viral tegument proteins

The previous bioinformatic analysis from our group by using the ExPASy ScanProsite tool showed that 27 HCMV tegument proteins comprise 74 potential linear PP1 binding motifs, precisely 63 RVxF motifs, 9 QVxF motifs and two SILK motifs [88]. With the knowledge that the RVxF motif is the most common, and that it occurs in most of the PP1 regulatory proteins [68], our next step was to test the protein-protein interaction between PP1 and the most abundant RVxF-containing viral tegument proteins using a M2H assay with full-length proteins. We investigated the PP1 interaction with three tegument proteins: UL24 and UL82 fused with GFP and UL38 including a C-terminal truncation ($UL38^{\Delta 831\text{-}931}$), but with an intact RVxF motif. However, in comparison to the positive control SDS22 we were not able to observe any luciferase activity upon co-transfection of PP1 and the tegument protein of interest (**Figure 9A**).

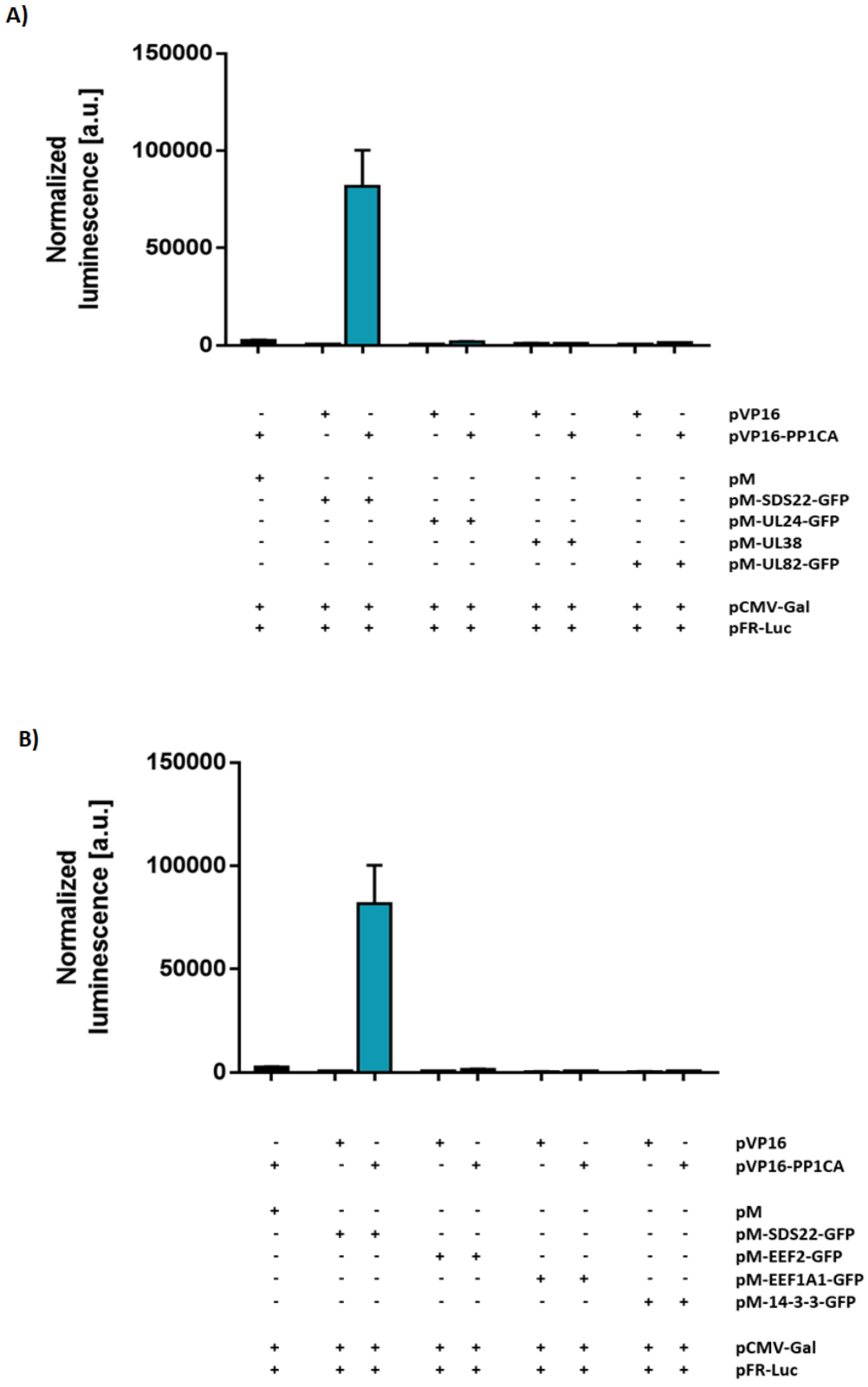

Figure 9) Interaction of tegument proteins with PP1α. The HCMV tegument proteins (A) and human proteins incorporated into HCMV tegument (B) were tested for interaction with PP1α in M2H assay.

HeLa cells were transfected with listed plasmids. pM-SDS22 represents positive control. Luciferase and β-galactosidase activities were measured 48h after transfection. The bars show luminescence normalized against β-galactosidase expression as a marker of transfection efficiency (mean ± SEM from technical triplicates). n=1.

The expression of the proteins was confirmed by using Western Blot, as well as by detection of GFP with fluorescence microscopy. We observed expression of all proteins in the cells, thus making the absence of a luminescence signal unlikely to be due to low transfection efficiency or impaired expression of transfected plasmids (**Figure 10, Figure 11**).

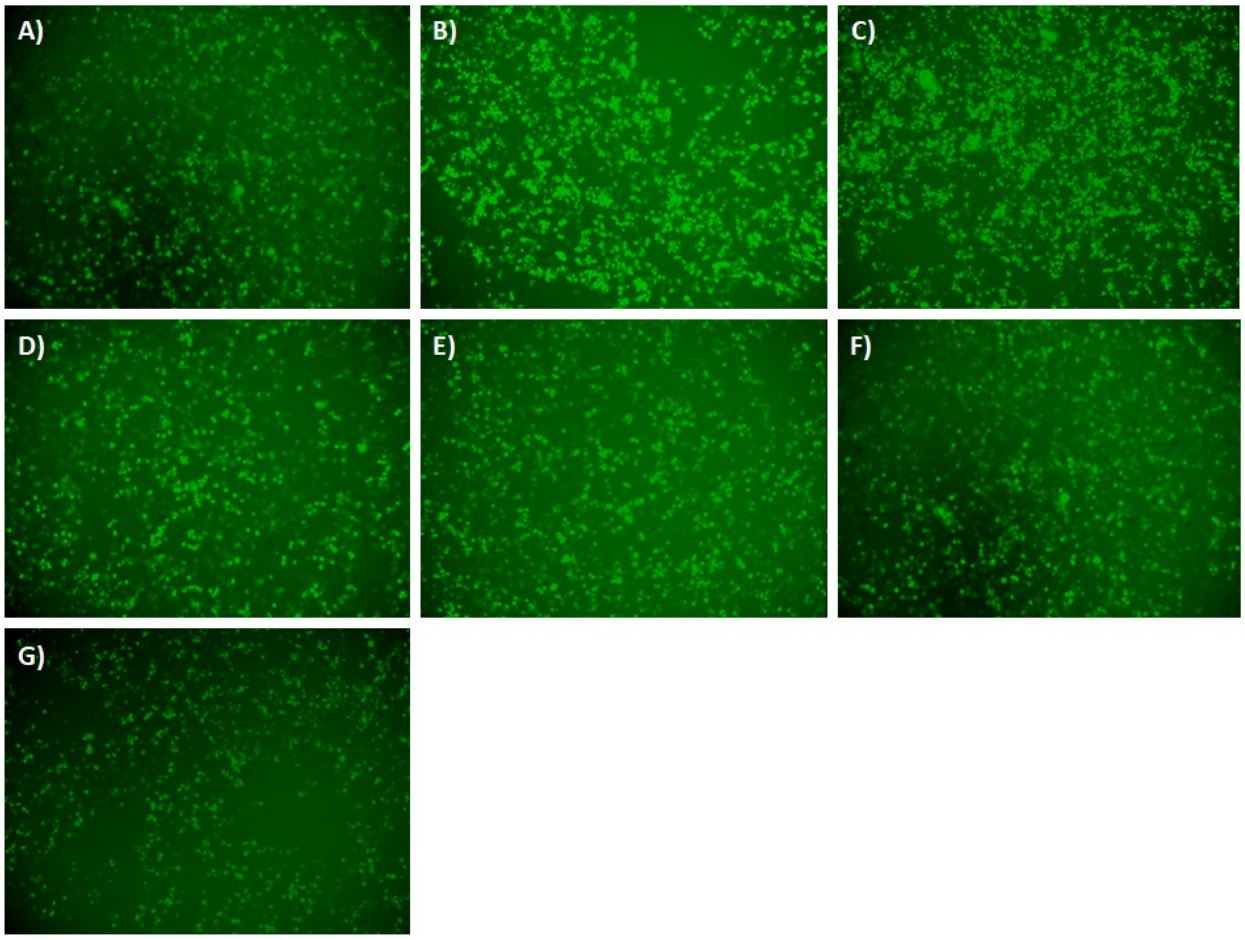

Figure 10) GFP expression in transfected HeLa cells. HeLa cells were transfected with pM-SDS22-GFP (A), pM-UL24-GFP (B), pM-UL82-GFP (C), pM-14-3-3-GFP (D), pM-EEF2-GFP (E), pM-EEF1A1-GFP (F) and pM-GRB2-GFP (G). GFP expression was observed by fluorescence microscopy. Images were taken using auto exposure.

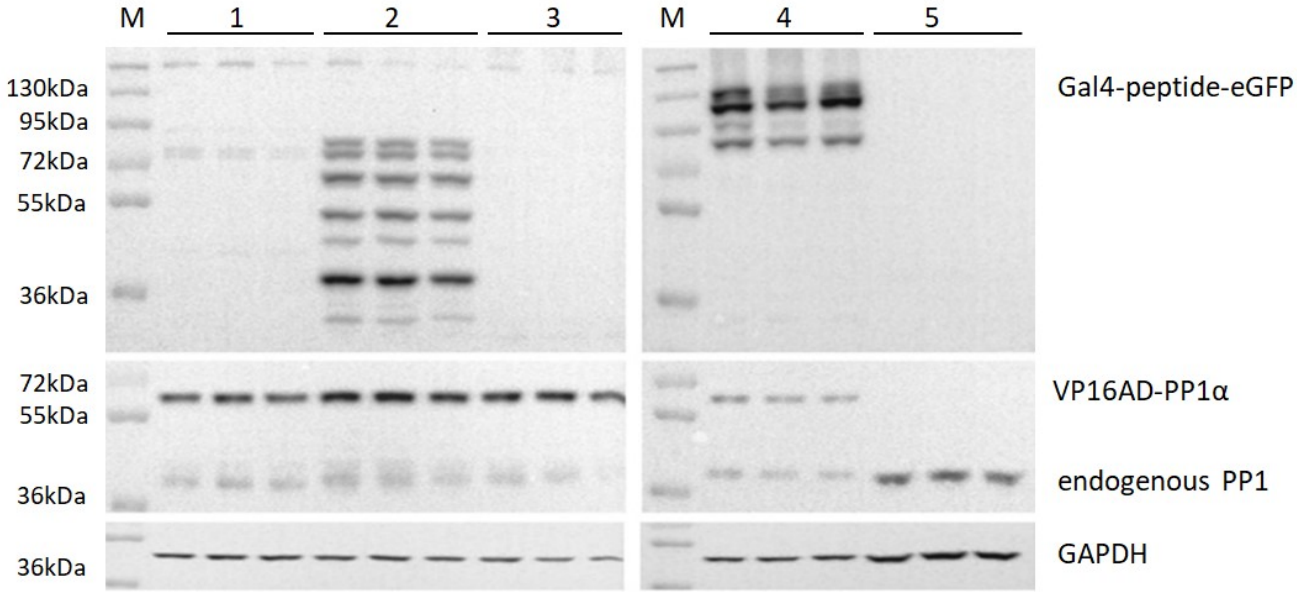

Figure 11) Detection of VP16AD-PP1 and HCMV proteins fused with GFP in lysates of transfected HeLa cells. HeLa cells were transfected for the M2H assay with pVP16-PP1CA and pM-SDS22-GFP (1), pVP16-PP1CA and pM-14-3-3-GFP (2), pVP16-PP1CA and pM-UL24-GFP (3) or pVP16-PP1CA and UL32-UL82-GFP (4). Untransfected cells were added as a negative control (5). PP1, GFP and GAPDH were detected using the respective monoclonal antibodies and HRP-linked secondary antibodies. M = marker, PageRuler Plus Prestained Protein Ladder.

5.3 Possible PP1 tegument incorporation as a human holoenzyme

Over 70 human proteins have been identified to be incorporated in the HCMV virions [52]. Considering that PP1 forms dimeric holoenzymes with more than 200 known cellular PP1 regulators [68], we hypothesized that PP1 can be incorporated as a human holoenzyme into the virus. Of all incorporated human proteins in the virus, 16 human proteins are determined as PP1 interacting proteins in the DEPOD database [89], (**Figure 12**). By a M2H, we tested the protein-protein interaction between PP1 and human proteins that co-occur in the virion tegument, including EEF2, EEF1A1 and 14-3-3. Our results show that none of these proteins induced luciferase expression compared to the positive control SDS22 (**Figure 9B**).

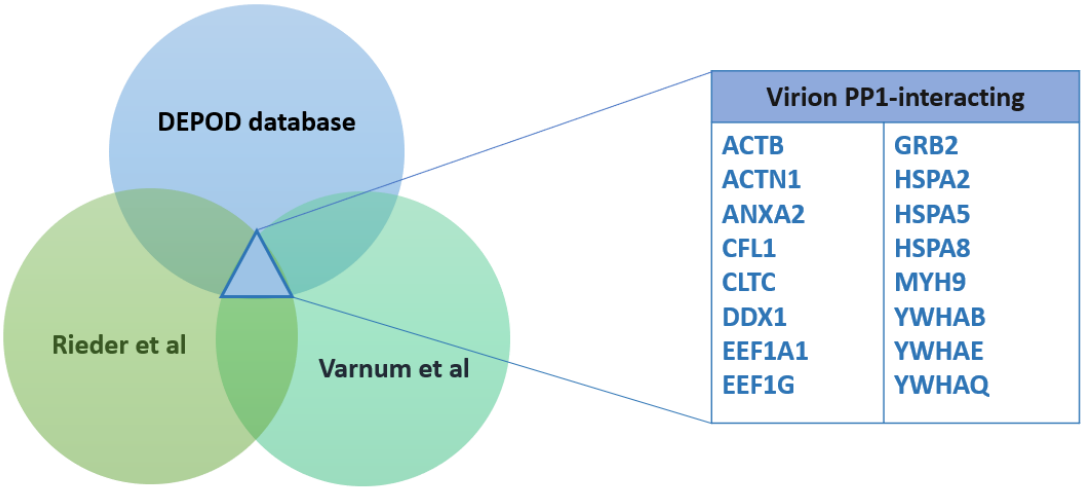

Figure 12) Human PP1 binding proteins in the HCMV tegument. The gene list of intersection between the indicated MS Datasets [52], [90] and the PP1 interactor list from DEPOD database [89].

It was previously reported that the incorporation of two cellular proteins, DDX3 and GRB2, in the viral particle depends on the major tegument protein pp65 [91]. Additionally, the PP1 incorporation into the tegument is reduced in the absence of pp65 [91]. DDX3 and GRB2 are furthermore determined as PP1-associated proteins in the DEPOD database [89]. Hence, we performed a M2H assay to test the interaction between PP1 and GRB2 in the presence or absence of pp65. For expression of pp65 in the cells, we transfected HeLa cells with pcDNA-pp65.

Our results show that GRB2 did not bind to PP1 directly in our assay, and the presence of pp65 had no impact on their interaction (**Figure 13**).

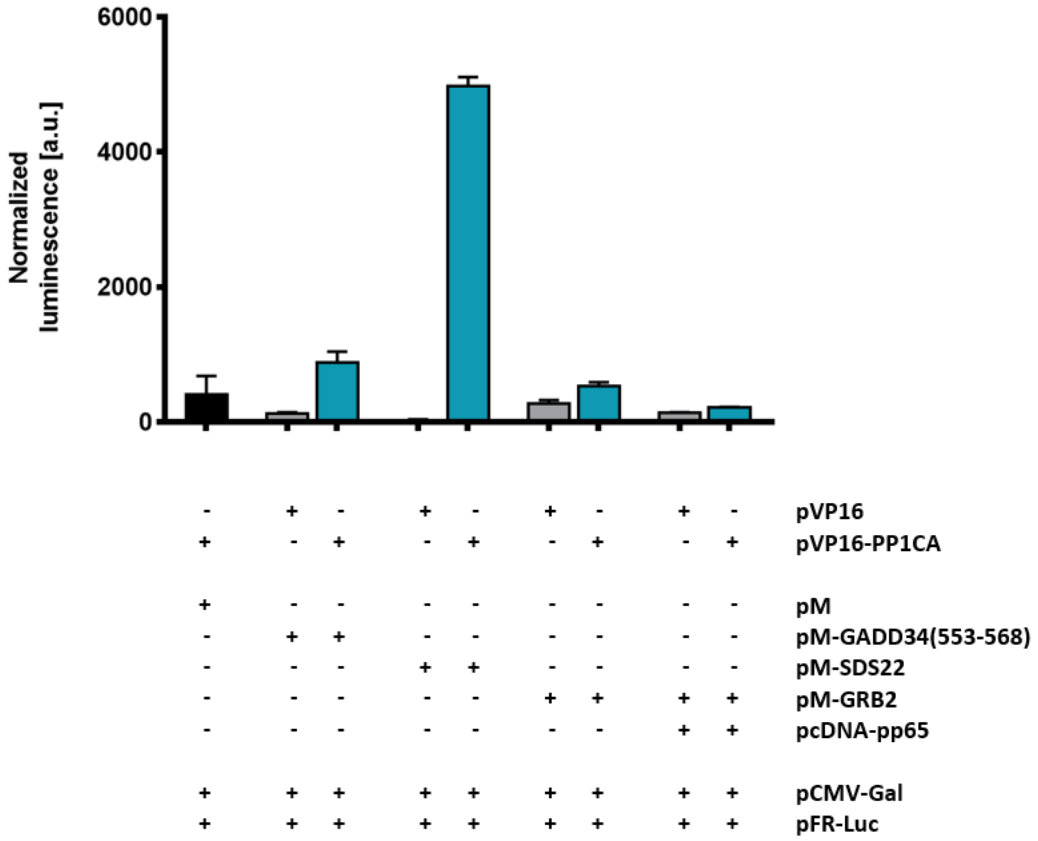

Figure 13) Interaction of PP1α and GRB2. GRB2 was tested for PP1 binding activity in the presence and absence of pp65 using M2H assay. HeLa cells were transfected with listed plasmids. pM-GADD34 (553-568) and pM-SDS22 represent positive controls. The numbers in brackets indicate the position of the first amino acid of the peptide within the protein. Luciferase and β-galactosidase activities were measured 48h post transfection. The bars show luminescence normalized against β-galactosidase expression as a marker of transfection efficiency (mean ± SEM from technical triplicates). n=1.

In order to confirm that the low luciferase activity is not a result of the absence of pp65 in the cells, we performed Western Blot analysis. As shown in **Figure 14**, pp65 was detectable in the cell lysates used for the M2H assays.

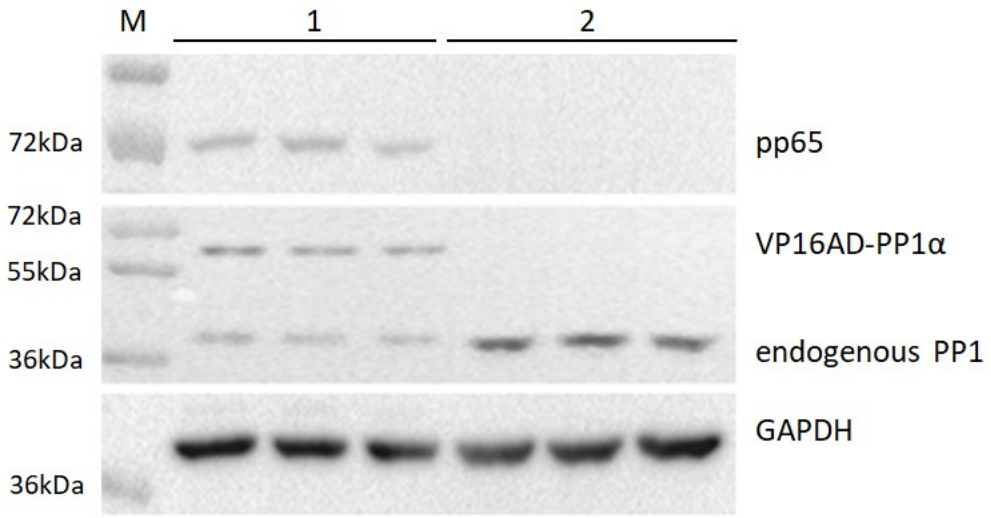

Figure 14) Detection of pp65 and VP16AD-PP1α expression in HeLa cells. HeLa cells were transfected for M2H assay with pVP16-PP1CA, pM-GRB2 and pcDNA-pp65 (1) or left untransfected (2). 48h after transfection, the cells were harvested and lysed followed by analysis by Western Blot. M = marker, PageRuler Plus Prestained Protein Ladder.

5.4 Co-immunoprecipitation

As we were unable to detect any direct binding of PP1 to viral tegument proteins and with the human proteins occurring in HCMV tegument, we decided to investigate potential complex formation of PP1 with viral tegument proteins. First, we investigated the possibility that pp65 binds to PP1 via other proteins in the cell using a Co-Immunoprecipitation (Co-IP). For a preliminary assay we used HeLa cells transfected with pcDNA-PP1 and pcDNA-pp65 and they were harvested by using a lysis buffer without SDS and EDTA. The proteins were immunoprecipitated with monoclonal α-PP1 and α-pp65 antibodies. As shown in **Figure 15A**, we could not detect complex formation with these two proteins (marked with red squares) under the conditions used. Additionally, we observed that the used PP1 monoclonal antibody was not very efficient in enriching PP1 from total lysate, while the pp65 monoclonal antibody showed better results (marked with yellow squares). It is important to note that we did not include a negative control IP using a nonbinding isotype control antibody in this preliminary experiment.

Next, we performed Co-IP including the positive control SDS22-GFP to ensure that our results are not caused by technical issues. The lysates were immunoprecipitated by using monoclonal α-PP1 antibodies and the Western blot was probed with α-GFP for detection of SDS22. However, PP1 staining in the IP

was weak and we could not detect the complex of PP1 with SDS22, indicating that the method is not established well. Also, GFP detection in the SDS22-GFP transfected sample input was hardly detectable (**Figure 15B**).

Although the used PP1 antibody is certified for IP by the manufacturer, we considered the possibility that the used monoclonal antibody against PP1 might cover the epitope required for binding to its interaction partner. To address this problem, we generated new vectors by site-directed mutagenesis containing PP1 fused to a His tag and SDS22 fused to a HA tag on their N-terminus. The HeLa cells transfected with these vectors were lysed by lysis buffer containing 1% NP-40 and 0.1% SDS and diluted 1:5 with 1xTBS for the overnight Co-IP reaction in order to reduce detergent concentration. As shown in **Figure 15C**, the complex PP1-SDS22 was successfully isolated only by using an anti-6x-His tag monoclonal antibody, while it was not detectable in the IPs with the HA-tag monoclonal antibody and PP1 monoclonal antibody. The possibility of antibody chain interference was excluded by including a mouse isotype IgG control IP reaction as well as the use of an α-light chain specific secondary HRP antibody for Western Blot detection.

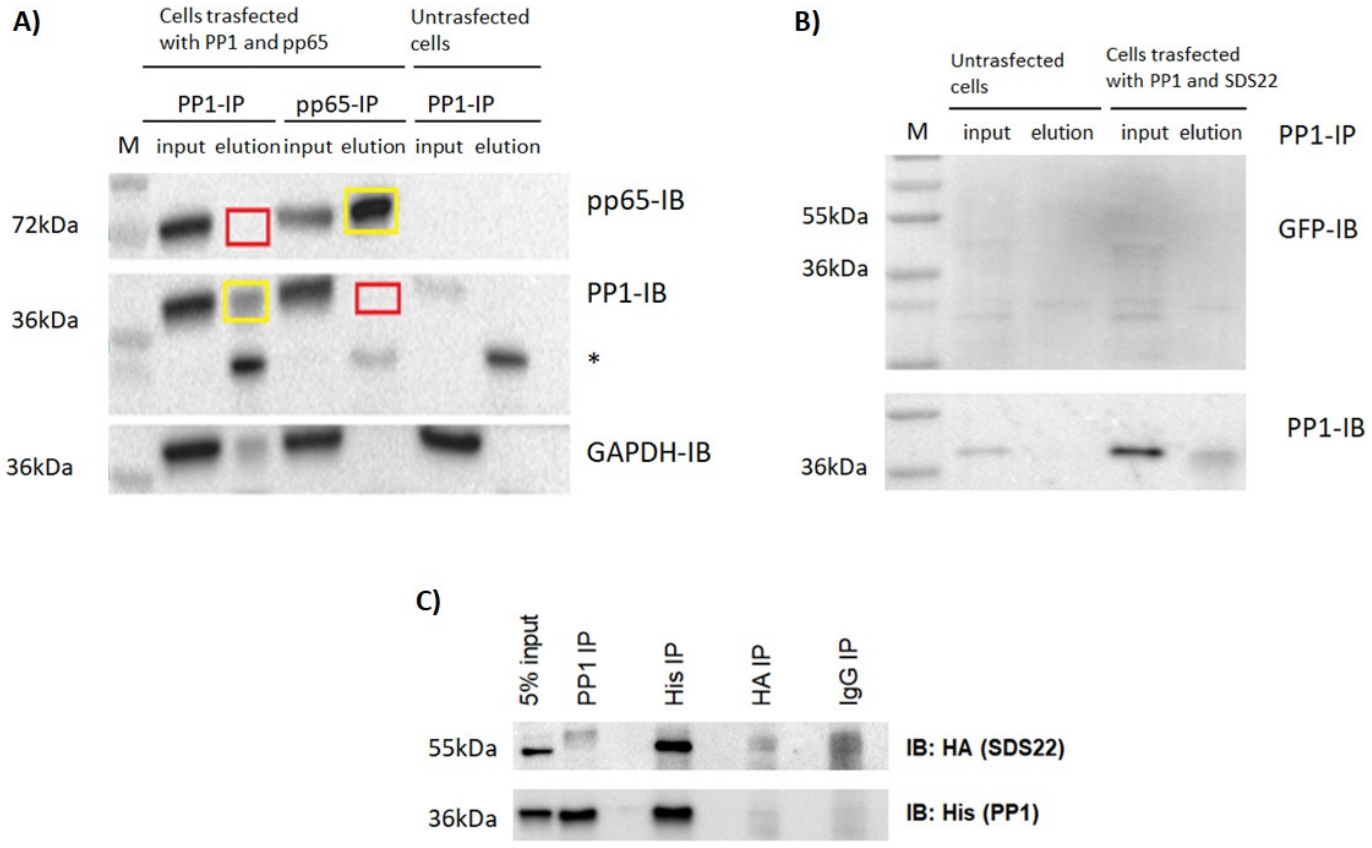

Figure 15) Western Blot analysis of Co-IP. A) HeLa cells were transfected with PP1 and pp65. The cells were harvested and lysed 48h post transfection. Immunoprecipitation (IP) was done with PP1 or pp65-specific antibodies and immunoblotting (IB) was performed with the indicating antibodies. Input samples correspond to 10% of the HeLa cell lysate used for IP. **B)** HeLa cells were cotransfected with PP1 and SDS22-GFP and were lysed 48h post transfection. The proteins were immunoprecipitated with PP1 antibody and the immunoblots were probed with PP1 and GFP antibodies. Input samples correspond to 10% of the HeLa cell lysate used in the assay. **C)** HeLa cells were transfected with His-PP1 and HA-SDS22. After 48h, cell lysates were immunoprecipitated with αHis, αHA or αPP1 antibodies followed by immunoblotting with the indicated antibodies. Mouse IgG was used as a control for nonspecific Co-IP. Input samples correspond to 5% of the HeLa cell lysate used for IP. For Western blot detection of proteins (IB), an α-light chain specific secondary antibody was used. M = marker, PageRuler Plus Prestained Protein Ladder. * α-light chain of secondary antibody

6 Discussion

It is already known that some human viruses such as HIV-1 and HSV-1 regulate PP1 activation in order to ensure their replication and spread of infection [92],[93]. Besides these viruses that use cellular PP1, it has been known that HCMV carries human PP1 in its own viral tegument[53], but so far the mechanism of PP1 incorporation as well as the role of the phosphatase in the virus particle are unknown. Recently, results from our group have confirmed the presence of PP1 in HCMV and additionally, PP1 was present at a higher concentration in virions compared to whole cell lysate of mock-infected and HCMV-infected fibroblasts (unpublished data). HCMV upregulates PP1 and its catalytic activity, leading to hypophosphorylation of host cell proteins within minutes of contacting the cell membrane, without any HCMV genome expression [53]. Taken all together, we can perceive an important role of PP1 for the life cycle of HCMV. Hence, our original hypothesis was that the incorporation of PP1 in the HCMV tegument is tightly regulated and can be mediated by at least one HCMV tegument protein by direct protein-protein interaction.

6.1 Validation of the interaction between PP1α and UL32

UL32 (pp150) was the first HCMV protein tested for PP1 interaction. It is a major phosphoprotein in the HCMV tegument and plays a role in capsid stability by binding multiple proteins, connecting the capsid with proteins of the assembly compartment. It has also been reported that UL32 is hypophosphorylated in the HCMV tegument [90]. This raises the possibility that the cellular phosphatases in the virion, such as PP1 and PP2A can lead to protein post-translational modifications within the virion tegument and thereby modulate viral infection. Moreover, UL32 contains several PP1 binding motifs, precisely four RVxF motifs and one SILK motif close to the RVxF motif “KVATF” at the C-terminus of the protein which is oriented toward the tegument in the viral particle. Considering that SILK is a rare PP1 binding motif which was found in only seven human PP1 regulators and does only occur in combination with RVxF [88], UL32 presented a promising candidate for PP1 binding.

According to previous research of our group, the peptide $UL32_{(997\text{-}1012)}$ containing the C-terminal RVxF motif can mediate an interaction with PP1 [88]. We investigated the specificity of this interaction by the generation of the mutated peptide $UL32_{(997\text{-}1012)\ KTAA}$ using a M2H assay. Our results showed that the mutated peptide $UL32_{(997\text{-}1012)\ KTAA}$ induced similarly low luciferase expression to the wild type UL32 peptide (**Figure 2**). Based on these results we can conclude that the originally observed signal is not dependent on an intact RVxF motif, making it likely that the peptide-PP1 interaction is unspecific. In

previous research of our group, GADD34$_{(553-568)}$ induced binding to PP1 and in this assay this peptide served as a positive control. GADD34$_{(553-568)}$ comprises a complete RVxF and ϕϕ motif which are both required for PP1 binding [80]. In comparison to the positive control, the UL32 peptides showed a lower luminescence signal. This difference might be due to the surrounding amino acids which probably impact the PP1 binding. Also, the signals obtained from peptide-PP1 interactions might be too weak to be robustly distinguished from background luminescence, and failed to induce luminescence in some cases of published PP1 interactors (e.g. HIV tat protein) in previous experiments [88].

Considering that secondary structures might be required for PP1 binding, we thus decided to test the possibility of direct binding between PP1 and full-length UL32. Besides UL32 wild type (UL32$_{WT}$), we wanted to test the interaction also with UL32 containing a mutated RVxF motif. For this purpose, we generated a KTVAF -> KTAAA (UL32$_{KTAAA}$) mutant using PCR-based site directed mutagenesis (**Figure 5**). In order to check their expression in the cells, we transfected the created plasmids into HEK293 cells, and the level of expression was checked 48h after transfection by Western Blot. We could observe similar expression of UL32$_{WT}$ and UL32$_{KTAAA,}$ suggesting that neither form was toxic to the cells, and the mutation did not prevent binding of the Western Blot antibody to the protein (**Figure 6**).

Next, we performed a M2H assay to investigate the interaction of PP1 and full-length UL32$_{WT.}$ For this assay we cloned the human protein SDS22 from cDNA into the pM vector, which served as positive control. SDS22, a PP1 regulator, contains twelve leucine-rich repeats (LRRs), which mediate the interaction with PP1. Interestingly, SDS22 can function as a ‘‘third’’ subunit of PP1 holoenzymes and prevent the autodephosphorylation of PP1 [76].

We could observe a strong luminescence signal in the positive control pM-SDS22-pVP16-PP1 transfected cells (**Figure 7B**). In contrast to the full-length positive control, the peptide GADD34$_{553-568}$ showed much lower luciferase expression, indicating that it might be more difficult to discern spurious interactions from stable protein-PP1 interactions using RVXF peptides only (**Figure 7B**). The peptide system was originally intended to be a cost- and time-effective way to screen multiple PP1-peptide interactions without the need of extensive cloning. Also, it can be useful to define which domain of a protein is included in the interaction with its binding partner [94]. However, the peptide binds to the protein via a smaller surface, which decreases the stability of the peptide-protein interaction [95]. Such unstable interaction can lead to the reduction of the luciferase expression, since the assay requires a stable interaction of the bait and prey proteins to function as a transcription factor for the luciferase gene. Additionally, previous research of our group has shown that GADD34$_{549-564}$ containing the full “KVRF”

sequence but a disrupted ϕϕ motif, has weaker luminescence signal than GADD34$_{553\text{-}568}$ [88]. These results indicate that the disruption of the ϕϕ motif decreased the binding affinity to PP1. Hence, we could see that the surrounding sequences can contribute to a peptide-protein interaction. In case of full-length proteins, the proteins assume their three-dimensional structure before their interaction as well as conformational changes during association, increasing the stability of the complex [95]. Hence, we conclude that a peptide-mediated screen for PP1-RVxF binding using a classical M2H approach is probably not appropriately reflecting the situation *in vivo*, and that full length proteins are more appropriate to discover PP1 interactors.

However, even when using the full-length protein, the results of our M2H assays did not show evidence that UL32 and PP1 are interaction partners (**Figure 7A-B**). In order to check UL32 expression in the cells, we performed Western Blot. Ul32 was expressed, but at a very low level (**Figure 8**). Part of the inability to properly detect UL32 could be the choice of lysis buffer used for the M2H assay. The M2H lysis buffer is optimized to solubilize the cytoplasmic luciferase without interfering with the assay reagents, whereas the interaction of the bait-prey transcription factor mainly happens in the nucleus. The positive control in **Figure 8** stems from HCMV-infected fibroblasts that were harvested in a different lysis buffer containing high salt and 0.1% SDS that might be more suitable to solubilize UL32. Also, the discrepancy between the observed fluorescence of cells transfected with GFP-fusion proteins (e.g. pM-SDS22-GFP) and Western Blot detection of GFP (**Figure 10**, **Figure 11**) suggests that the Western Blot lysates using M2H lysis buffer do not accurately represent the cellular content of the detected proteins.

Secondly, the fact that UL32 is a large protein of 150kDa might negatively impact the transfection of the cells or require longer incubation times for proper expression. In order to see whether longer incubation time is required to improve UL32 expression, we performed an additional M2H assay where we used lysates of UL32-transfected cells incubated for 72h after transfection. Again, UL32 expression via Western Blot was hardly detectable (data not shown).

We also tested C-terminal fragments of UL32$_{437\text{-}1048}$ for interaction with PP1. We could not observe luciferase expression in the PP1:UL32$_{437\text{-}1048}$ combination compared to GADD34$_{553\text{-}568}$ (**Figure 7A**). Considering that full-length UL32 and UL32cterm are not fused with GFP, we could not detect their expression by fluorescence microscopy. The C-terminal fragment was weak detectable by Western Blot, but we noticed the presence of smaller bands in the UL32$_{437\text{-}1048}$ lysates, suggesting a possible degradation of the protein (**Figure 8**).

Before making conclusions about the M2H assay, the interaction of UL32 with PP1 has to be confirmed by some other assay suitable for the detection of protein-protein interaction. One of the possibilities can be the use of the NanoBiT® system (Promega), where the proteins of interest would be fused with Nano Bit subunits instead a reporter gene. In addition to the NanoBit technology, bimolecular fluorescence complementation (BiFC) assays are widely used for the identification of protein-protein interaction. These assays would probably be more suitable for the detection of transient and weak interactions. Another possibility to stabilize weak interactions would be the use of a catalytic "substrate trap" variant, i.e. PP1 mutant with an inactive catalytic domain.

6.2 Investigation of PP1 binding by other HCMV tegument proteins

PP1 is characterized by the presence of several docking motifs, RVxF, SILK, MyPhoNE, SpiDoC and IDoHA [68]. All known tegument protein sequences were screened for the presence of the PP1 binding motifs RVxF, QVxF, SILK and MyPhoNE. 74 PP1 binding motifs in 37 HCMV tegument proteins have been detected, the RVxF motif alone occurring in as many as 27 tegument proteins [88]. The RVxF-type docking motif is present in nearly 90% of the validated PP1 interactors [68], hence we decided to test the interaction between virion tegument proteins containing RVxF and PP1 in addition to UL32. Since we established that the peptide system was not feasible to identify PP1 interactors, we next tested the interaction with full-length tegument proteins.

We furthermore investigated the three virion proteins UL24, UL38 and UL82 in a M2H assay. We could not confirm PP1 binding for any of these tegument proteins (**Figure 9A**). These are examples that the mere presence of PP1 binding motifs does not necessarily predict binding to PP1, although the majority of PP1 regulators and substrates interacts with PP1 via the RVxF motif [65]. In addition, the RVxF motif is a very short linear motif with a high probability of occurring randomly.

In the case of UL38, we were unable to clone the full-length protein from the cDNA of infected cells. Thus, the low luminescence signal might be caused by the presence of the deletion, although the RVxF motif is not damaged in the truncated protein. On the other hand, in the pM-UL38 vector UL38 is not fused with GFP due to cloning restrictions. Because of a lack of commercially available antibodies against UL38 we were thus unable to verify its expression in the cells.

UL38 inhibits the host apoptosis and facilitates efficient viral replication [32]. McKinney et al. found that UL38 increases the level of EEF2 and PP1 catalytic subunit in response to either HCMV-infection or UL38-

induction in uninfected cells. Additionally, upon infection with an HCMV strain with deleted UL38, the amount of EEF2 and PP1 in the cell is decreased [96]. These findings highlight a role of UL38 in regulating PP1 and indicate that UL38 may promote translation during HCMV infection. EEF2 is completely inactivated in the phosphorylated state [97], it would thus be interesting to investigate whether UL38 induces the dephosphorylation and activation of EEF2 by PP1. Hence, UL38 can regulate the maintenance of translation elongation during HCMV infection [98]. Taken all together, UL38 represents one of the important candidates for the investigation of the interaction with PP1, while PP1 may be an important regulator in the translation of viral proteins during infection.

As already mentioned earlier, UL82 is involved in the cGAS-STING pathway: it inhibits the recruitment of the cellular kinases TBK1 and IRF3 to the STING complex and thereby suppresses antiviral gene expression [41]. Preliminary data of our group also showed that PP1 is involved in this signaling cascade. Primary human foreskin fibroblasts infected with HCMV have shown a significant increase in phosphorylated IRF3 and STING in the presence of a noncatalytic PP1-inhibitor (unpublished data). These findings indicate an important role of PP1 in the cGAS/STING cascade, which might be mediated by UL82. Although our results have shown that there is no direct interaction of PP1 and UL82, still it is necessary to further investigate whether a complex involving these two proteins might be formed and thus regulate cGAS-STING signaling.

6.3 PP1 incorporation in HCMV as holoenzyme

Multiple studies have shown that HCMV integrates over 70 human proteins into its tegument [52], [90]. Of all incorporated human proteins in the virus, 16 human proteins are determined as PP1 binding proteins in DEPOD [89], a manually curated database harboring information about phosphatase substrates and protein interaction partners. Since PP1 acts as a holoenzyme, we next considered the possibility that PP1 might be incorporated into the tegument as a fully human complex together with its regulatory protein.

Interestingly, the group of human PP1 binding proteins occurring in the viral tegument also contains translation elongation factors, including also EEF2, which plays a central role in translation elongation and, as mentioned earlier, is regulated by the HCMV UL38 protein during infection [96]. We thus aimed to test the protein-protein interaction between PP1 and human virion tegument proteins, including the elongation factors EEF2, EEF1A1 and the scaffold protein 14-3-3. Our result show that PP1 does not directly interact with these proteins in the M2H system (**Figure 9B**). However, the process of

dephosphorylation can occur briefly, as it happens with most of the proteins involved in biochemical cascades [99], making it possible to miss weak interactors. The M2H assay is a convenient method for the detection of the stable interactions between proteins and thus might miss transient phosphatase-substrate interactions. Additionally, the cells could shape signaling depending on the stimuli that they receive. Some proteins may not fold properly if they are not in their natural physiological environment, which can negatively impact protein-protein interactions [100]. Considering that the bait proteins are fused with the Gal4 DNA binding domain and GFP to detect their expression in the cells, the reporter protein could cause steric hindrance and prevent protein interactions [101]. Besides these factors that can affect the protein-protein interaction in the artificial M2H system, it would be necessary to apply some additional methods to investigate the interaction with PP1 before making a conclusion.

Our next attempt was the investigation of the interaction between PP1 and GRB2. It has been shown that the incorporation of two cellular proteins, DDX3 and GRB2 in the viral particle depends on the major tegument protein pp65 [91]. Interestingly, supplementary data provided by Cavignac et al. also suggest that PP1 incorporation into the tegument is less efficient in the absence of pp65 [91]. Also, DDX3 and GRB2 are determined as PP1-associated proteins in the DEPOD database [89], therefore they became our next candidates for the M2H assay. However, we were not able to subclone pp65 and DDX3 into the appropriate pM-fused M2H vector due to restriction site incompatibilities. Therefore, we only tested the direct interaction between PP1 and GRB2 as well as the possibility that the presence of pp65 (which does not contain any primary PP1 binding motifs) might influence their interaction. The expression of pp65 was enabled by co-transfection of pcDNA-pp65. In comparison to the positive control SDS22, we were not able to observe any luciferase activity upon co-transfection of PP1 and GRB2. Furthermore, the presence of pp65 did not have any impact on their interaction (**Figure 13**). We detected the expression of pp65 in the cells by Western Blot, indicating that the low luminescence signal is not caused by the absence of pp65 in the cells (**Figure 14**).

pp65 is involved in the manipulation of the host's immune system and it is the major constituent of both virions and dense bodies [102]. pp65 inhibits the activation of IRF-3 within early times after infection. IRF-3 is the important transcription factor needed to initiate an IFN-α/β response, which is a key component of the cell's innate immune response. An analysis has shown that pp65 promotes the dephosphorylation and export of IRF-3 without forming a stable interaction [49], [103]. Considering that PP1 targets IRF3 which results in a suppression of IFNβ production [104], and pp65 is

hypophosphorylated during HCMV infection [90], it would be indeed interesting to further explore the direct or indirect interaction between pp65 and PP1.

In order to ensure that the low luciferase activity in M2H assays is not due to poor transfection efficiency or expression of the fusion proteins, we performed Western Blot analysis by using lysates of transfected cells. PP1 was almost equally expressed in all samples, while the detected amounts of GFP were highly variable indicating that the fusion protein is not or only poorly expressed in some samples (**Figure 4**, **Figure 11**). This might be caused by technical issues like protein degradation during sample preparation. There is also the possibility that fusion proteins were only insufficiently isolated, because the fusion protein is supposed to be predominantly located in the nucleus whereas the cell lysis approach for M2H assays mainly aims to isolate cytoplasmic luciferase. The positive control SDS22 together with PP1 is localized mostly at the kinetochore in nucleus [105] and we were able to detect a robust luminescence signal upon co-transfection PP1-SDS22. Proteins that are naturally localized in the nucleus might thus be predestined to give a more robust signal than proteins that harbor other localization signals. Additionally, we observed comparable GFP expression between samples by fluorescence microscopy which clearly confirmed the expression of fusion proteins (**Figure 3**, **Figure 10**). These results indicate that negative signals were not due to poor expression of the fused proteins. However, we did not account for differences in protein localization, which may greatly impact the effectivity of the bait-prey transcription factor in binding to the luciferase promoter.

6.4 Co-immunoprecipitation

So far, we aimed to find a viral tegument protein or human protein incorporated into the viral tegument which directly binds to PP1 in a M2H assay. However, besides binary protein-protein interactions, several proteins can be included in the same biological process and act as a protein complex. That led us to the idea that PP1 might be part of a bigger complex also containing HCMV proteins. For this purpose, we first performed a co-immunoprecipitation in order to find out whether PP1 is in a complex with pp65. As mentioned earlier, PP1 incorporation into the tegument seems to depend on pp65 [91], making it a very interesting candidate. In a preliminary co-immunoprecipitation experiment, we transfected HeLa cells with pcDNA-PP1 and pcDNA-pp65 and harvested proteins in a lysis buffer without SDS and EDTA in order to minimize disruption of protein-protein interactions. The protein complexes were immunoprecipitated by either α-PP1 or α-pp65 antibodies coupled with protein A/G beads. We were not able to detect that these two proteins form a complex (**Figure 15A**). Additionally, the used PP1 monoclonal antibody was not very efficient in enriching PP1 from total lysate, while the pp65

monoclonal showed a better enrichment compared to the input before IP. Importantly, in this first experiment no negative control was included, making the interpretation of co-eluted proteins problematic. In order to ensure that our negative results are not due to technical issues, we first included SDS22 as a positive control in the next Co-IP assay. However, we could not detect the complex of PP1 with SDS22 in an initial experiment, indicating that the method is not established well and requires further optimization (**Figure 15B**).

It is possible that the used monoclonal antibody against PP1 covers the epitope required for binding of its interaction partner. Therefore, we created a new vector containing PP1 fused to a His tag and SDS22 fused to a HA tag on their N-terminus. We also changed to a lysis buffer containing 1% NP-40 and 0.1% SDS in order to improve lysis and protein solubilization from the nucleus. After lysis and for the duration of the antibody incubation, the lysis buffer was then diluted 1:5 with 1xTBS in order to dilute detergent and better preserve protein-protein interactions. This proved to be a better option since we could successfully isolate the complex PP1-SDS22 by using an anti-6x-His tag monoclonal antibody for IP, while neither IP nor Co-IP not possible with the HA-tag monoclonal antibody used (**Figure 15C**). Considering the positive results by using an Anti-6x-His tag monoclonal antibody, we will continue with the investigation of protein complexes with His-PP1. pp65 and UL38, which were mentioned earlier as regulators of PP1 targets, should be among the first candidates to test.

6.5 Outlook

The survival of viruses depends on molecular protein-protein interactions with their hosts, indicating that the comprehension of virus-host interaction is essential for the understanding of viral infection mechanisms and the development of new drugs [106].

In this work, we aimed to find mechanisms of PP1 incorporation into the HCMV particle by investigating the interaction between PP1 and HCMV tegument proteins. Our results showed that none of the tested HCMV tegument proteins and human proteins could directly bind PP1 with the methods used. Despite the detection of the positive control SDS22, we have to consider technical reasons for the absence of signal. Perhaps different steps in the M2H assay, such as the reporter genes, plasmid copy number, lysis buffer, folding of fusion proteins could have an impact on the outcome of the experiment. In order to confirm protein-protein interaction, different assays for the detection of protein-protein interactions must be performed additionally. Considering that M2H is only useful for the investigation of direct interactions, our aim was to examine the possibility that PP1 can form a complex with HCMV tegument

proteins, for which we used Co-immunoprecipitation assays. We successfully optimized Co-IP using the cells transfected with PP1 and SDS22 fused with tags and the PP1 complex was immunoprecipitated by Anti-6x-His tag monoclonal antibody. In future experiments, Co-IP can thus be used for testing our candidate proteins as PP1 binders, with the caveat that Co-IP assays are technically challenging and must be optimized for every antibody or interaction. Another shortcoming of the performed assay is the use of HeLa cells with artificially overexpressed proteins which might not adequately reflect the situation during infection.

Therefore, it would be also interesting to perform endogenous Co-IP with HCMV infected cells. For this purpose, it will be necessary to use an appropriate PP1-targetintg antibody for immunoprecipitation, because so far, we have had poor success with transfection and protein overexpression in primary human foreskin fibroblasts which are used for propagation of HCMV. This way, it would be possible to detect the interaction between PP1 and viral proteins, which might bind to the PP1 complex only in certain conformational states induced during infection. This might theoretically be the case with UL32, that contains the rare PP1 binding motif SILK, which occurs only in combination with RVxF motif.

Finally, the coupling of Co-IP with peptide-based mass spectroscopy (MS) will allow the identification of PP1 interactome and its changes during HCMV infection in comparison to noninfected human foreskin fibroblasts (HFF).

7 Zusammenfassung

Das Humane Cytomegalievirus (HCMV) ist ein verbreitetes Pathogen, das lebenslange Infektionen hervorruft und in immunkompromittierten Patienten Komplikationen verursacht. HCMV trägt die humane Proteinphosphatase 1 (PP1), welche es von infizierten Zellen erbeutet, in der Tegumentschicht des Virions mit. Es ist bisher unklar, welche biologische Konsequenz daraus resultiert und welche molekularen Mechanismen dahinterstecken.

Der Zweck dieser Arbeit war es herauszufinden, welche HCMV Tegumentproteine an PP1 binden. Bereits in einer früheren Studie unserer Gruppe wurde UL32 als Bindekandidat (über ein kurzes RVxF Motiv) identifiziert. Mittels Mutagenese und Mammalian 2hybrid (M2H) Assays konnten wir nun allerdings nachweisen, dass dieses schwache Signal wahrscheinlich keine spezifische Interaktion über RVxF darstellt. Außerdem wiesen wir nach, dass sich peptidbasierte Anwendungen in der Identifikation von PP1 Bindungspartnern via M2H weniger gut eignen als Proteine in voller Länge. Allerdings konnten wir auch mit den Gesamtproteinen UL24, UL32, UL38 und UL82 von HCMV keine Interaktion nachweisen. Mehrere Massenspektrometriedatensätze geben zudem Hinweise darauf, dass HCMV zusätzliche humane Proteine im Virion mitträgt, von denen manche potenziell mit PP1 interagieren, was eine mögliche Inkorporation von PP1 als komplett humanes Holoenzym suggeriert. Die vier humanen Proteine die wir hierzu testeten, gaben zunächst keinen Hinweis auf eine direkte Interaktion über M2H oder ersten Co-Immunopräzipitationsversuchen (Co-IP).

Abschließend haben wir ein Protokoll für die Co-IP von His-markiertem PP1 mit HA-SDS22 und anderen potenziellen PP1-Bindern optimiert. Diese Methode wird weiter zur Identifizierung von viralen PP1-Interaktoren beitragen, sowie zur Aufklärung des molekularen Mechanismus der PP1-Integration beitragen.

8 Appendix

8.1 Materials (extended)

8.1.1 Consumables

Table 8) List of consumables with company name and product number.

Reagent	Company	Product number
10% SDS Solution	Bio-Rad	#1610416
2-Mercaptoethanol	Sigma-Aldrich	M6250
2-Nitrophenyl β-D-galactopyranoside (ONPG)	Sigma	N1127
30% Acrylamide/ Bis solution	Bio-Rad	1610154
50x Tris / Acetic Acid / EDTA (TAE), Nucleic Acid Electrophoresis	Bio-Rad	1610743
Agar-Agar	Merck	101614
Ampicillin Sodium Salt	Sigma-Aldrich	A9518
Biozym LE Agarose	Biozym	840004
Dimethyl sulfoxide (DMSO)	Sigma-Aldrich / Merck	D8417-100ML
Ethylenediaminetetraacetic acid disodium salt dihydrate (EDTA)	Sigma-Aldrich	E5134
GelRed® Nucleic Acid Gel Stain, 10,000x	Biotium	41003
Glycerol	Merck	356350
Halt™ Protease and Phosphatase Inhibitor Cocktail (100x)	Thermo Scientific™	78440
Luciferase Cell Culture Lysis 5x Reagent	Promega	E1500
Orange G (for NA electrophoresis)	Sigma-Aldrich	O3756
PageRuler Plus Prestained Protein Ladder	Thermo Scientific™	26618
PBS-Puffer, pH 7,4 - 10x Konzentrat	Morphisto	11237
Pierce™ Bovine Serum Albumin Standard Pre-Diluted Set	Thermo Scientific™	23208
Pierce™ 660nm Protein Assay Reagent	Thermo Scientific™	22660
Quick-Load® 1kb DNA Ladder	New England BioLabs	NO468S
S.O.C Medium	Invitrogen™	15544034
Sodium chloride	Sigma-Aldrich	S7653
Sodium dodecyl sulfate (SDS)	Sigma-Aldrich	436146
Subcloning Efficiency™ DH5α™ Competent Cells	Invitrogen™	18265017
Tris(hydroxymethyl)aminomethane	Sigma-Aldrich	252859

Trypan Blue Solution, 0.4%	Gibco™	15250061
Tryptone	Sigma-Aldrich	T7293
TWEEN 20	Sigma-Aldrich	P7949

8.1.2 Plates and flasks

Table 9) List of plates and flasks used for mammalian two-hybrid assays, cell cultivation and for LB-agar plates.

Article	Company	Product number
96-well Black/Clear Flat Bottom Microplate	Corning®	353219
CELLSTAR 96 well plates (clear plates)	Greiner Bio-One International	655180
CELLSTAR Zellkultur Multiwellplatte, 24 wells	Greiner Bio-One International	662160
CELLSTAR Zellkultur Multiwellplatte, 6 wells	Greiner Bio-One International	657160
Cellstar Zellkulturflasche 250ml, 75cm2	Greiner Bio-One International	658175
Nunc™ Cell Culture/Petri Dishes	Thermo Scientific™	172931
Falcon™ Bacteriological Petri Dishes	Thermo Scientific™	10720052

8.1.3 Cell culture

Table 10) List of reagents required for cell cultivation.

Article	Company	Product number
0,05% Trypsin-EDTA (1x)	Gibco™	23300-062
Antibiotic-Antimycotic (100x)	Gibco™	15240062
DPBS (1x) Dulbecco's Phosphate Buffer Saline	Gibco™	14190-094
Fetal Bovine Serum, qualified, heat inactivated	Gibco™	10500-064
TurboFect Transfection Reagent	Thermo Scientific™	R0531

8.1.4 Co-Immunoprecipitation

Table 11) Beads used for immunoprecipitation.

Article	Company	Product number
Protein A/G PLUS-Agarose	Santa Cruz Biotechnology	sc-2003

8.1.5 Western Blot

Table 12) List of and materials required for Wet Western Blots.

Article	Company	Product number
PageRuler™ Plus Prestained Protein Ladder, 10 to 250 kDa	Thermo Scientific™	26619
PVDF Transfer Membrane	Thermo Scientific™	88518
Restore™ PLUS Western Blot Stripping Buffer	Thermo Scientific™	46430
StartingBlock™ (PBS) Blocking Buffer	Thermo Scientific™	37538
SuperSignal™ West Femto Maximum Sensitivity Substrate	Thermo Scientific™	34096
SuperSignal™ West Pico PLUS Chemiluminescent Substrate	Thermo Scientific™	34096
SuperSignal™ West Pico PLUS Chemiluminescent Substrate	Thermo Scientific™	34577

8.1.6 Polymerase Chain Reaction

Table 13) List of materials for polymerase chain reactions (PCR). iProof™ High-Fidelity DNA Polymerase and iTaq™ DNA Polymerase Kits provide all necessary buffers, MgCl2 and DMSO.

Article	Company	Product number
dATP Solution (100mM)	Thermo Scientific™	R0141
dCTP Solution (100mM)	Thermo Scientific™	R0151
dGTP Solution (100mM)	Thermo Scientific™	R0161
dTTP Solution (100mM)	Thermo Scientific™	R0171
iProof™ High-Fidelity DNA Polymerase, 100U	Bio-Rad	1725301
iTaq™ DNA Polymerase	Bio-Rad	1708870

8.1.7 Kits

Table 14) List of kits required for protein concentration measurement, plasmid preparation, gel extraction, PCR purification, RNA isolation and cDNA synthesis.

Article	Company	Product number
Pierce™ BCA Protein Assay Kit	Thermo Scientific™	23225
QIAprep Spin Miniprep Kit (250)	Qiagen	27106
QIAGEN Plasmid Midi Kit (25)	Qiagen	12143
QIAGEN Plasmid Maxi Kit (25)	Qiagen	12163
QIAquick Gel Extraction Kit (250)	Qiagen	28706
QIAquick PCR Purification Kit (250)	Qiagen	28106
PureLink™ RNA Mini Kit	Invitrogen	12183020
iScript™ cDNA Synthesis Kit	Bio-Rad	1708890

8.1.8 Enzymes

Table 15) List of restriction enzymes and ligase with appropriate buffers.

Article	Company	Product number
FastDigest BamHI	Thermo Scientific™	FD0054
FastDigest EcoRI	Thermo Scientific™	FD0274
FastDigest XbaI	Thermo Scientific™	FD0684
FastDigest KpnI	Thermo Scientific™	FD0524
FastDigest NheI	Thermo Scientific™	ER0971
FastDigest DpnI	Thermo Scientific™	FD1703
FastDigest Buffer (10x)	Thermo Scientific™	B64
T4 DNA Ligase	Promega	M180A / M180B
T4 DNA Ligase 10x Buffer	Promega	C126B

8.2 List of abbreviations

4E-BP1	Eukaryotic translation initiation factor 4E binding protein 1
AC	Assembly complex
ATF4	Activating transcriptional factor 4
BicD1	Bicaudal D1
BiFC	Bimolecular fluorescence complementation
CCMV	Chimpanzee cytomegalovirus
cGAS	Cyclic GMP-CMP synthase
Co-IP	Co-immunoprecipitation (Co-IP) assays
CREB	Cyclic adenosine monophosphate (cAMP) response element-binding protein)
CTL	Cytotoxic T lymphocytes
EBOV	Ebola virus
eIF2α	Eukaryotic translation initiation factor 2α
eIF4F	Eukaryotic translation initiation factor 4F
GADD34	Growth-arrest- and DNA damage-induced transcript 34
HBV	Hepatitis B virus
HBx	X regulatory protein
HCMV	Human cytomegalovirus
HDACs	Histone deacetylases
HEXIM1	Hexamethylene bisacetamide-inducible protein 1
HFF	Human foreskin fibroblasts
HHV-5	Human herpesvirus 5
IRF-3	Interferon regulatory factor 3
LRRs	Leucine-rich repeats
M2H	Mammalian 2 hybrid assays
MCMV	Murine cytomegalovirus
MHC	Major histocompatibility complex
MIEP	Viral major IE promoters
MS	Mass spectroscopy
MTOC	Microtubule organizing center

mTORC1	Mammalian target of rapamycin complex 1
MyPhoNE	Myosin phosphatase N-terminal element
NK	Natural killer
PABA	Poly(A) binding protein
Plk1	Polo-like kinase 1
PP1	Protein Phosphatase 1
PP1C	Protein phosphatase 1 catalytic subunit
PPM	Metallo-dependent protein phosphatase
PPP	Phosphoprotein phosphatase
P-TEFb	Positive transcription elongation factor
PTP	Protein-tyrosine phosphatase
RNAPII	RNA polymerase II
SDS22	Suppressor of Dis2 mutant 2
Ser/Thr	Serine / threonine
SLiMs	Short linear motifs
TBK1	TANK binding kinase 1
TSC2	Tuberous sclerosis protein 2
USP24	Ubiqui+A2:B48tin-specific protease 24

8.4 List of tables

8.5 List of figures

9 References

[1] R. Seitz, “Human Cytomegalovirus (HCMV)-Revised,” *Transfus. Med. Hemotherapy*, vol. 37, no. 6, pp. 365–375, 2010.

[2] J. Paul and T. Iii, “Human cytomegalovirus tegument proteins Human cytomegalovirus tegument proteins,” vol. 22, no. January, 2012.

[3] E. Poole, M. Wills, and J. Sinclair, “Human Cytomegalovirus Latency : Targeting Differences in the Latently Infected Cell with a View to Clearing Latent Infection,” vol. 2014, 2014.

[4] S. E. Jackson *et al.*, “CONFERENCE PROCEEDINGS CMV immune evasion and manipulation of the immune system with aging,” pp. 273–291, 2017.

[5] H. Buxmann, K. Hamprecht, M. Meyer-wittkopf, and K. Friese, “Primary Human Cytomegalovirus (HCMV) Infection in Pregnancy,” pp. 45–52, 2017.

[6] D. A. Ortiz, “The Roles Of Human Cytomegalovirus Tegument Proteins Pul48 And Pul103 During Lytic Infection,” 2016.

[7] A. Carlson, E. R. Norwitz, and R. J. Stiller, “Cytomegalovirus Infection in Pregnancy : Should All Women Be Screened ?,” vol. 3, no. 4, pp. 172–179, 2010.

[8] M. G. Revello and G. Gerna, “Diagnosis and Management of Human Cytomegalovirus Infection in the Mother , Fetus , and Newborn Infant,” vol. 15, no. 4, pp. 680–715, 2002.

[9] M. Dietrich and J. Schieffelin, “Congenital cytomegalovirus infection,” *Ochsner J.*, vol. 19, no. 2, pp. 123–130, 2019.

[10] B. A. Krishna and J. H. Sinclair, “Advances in the treatment of cytomegalovirus,” no. October, pp. 5–17, 2019.

[11] T. Crough and R. Khanna, “Immimobiology of human cytomegalovirus: From bench to bedside,” *Clinical Microbiology Reviews*, vol. 22, no. 1. pp. 76–98, Jan-2009.

[12] E. Forte, Z. Zhang, E. B. Thorp, M. Hummel, and M. Hummel, “Cytomegalovirus Latency and Reactivation : An Intricate Interplay With the Host Immune Response,” vol. 10, no. March, 2020.

[13] Y. Wang, X. Zhao, and S. E. Jackson, “Human Cytomegalovirus Primary Infection and Reactivation : Insights From Virion-Carried Molecules,” vol. 11, no. July, 2020.

[14] T. Transcriptome, H. Cytomegalovirus, M. Schwartz, and N. Stern-ginossar, “The Transcriptome of Latent Human Cytomegalovirus,” no. January, pp. 1–7, 2019.

[15] R. F. Kalejta, “Tegument Proteins of Human Cytomegalovirus,” vol. 72, no. 2, pp. 249–265, 2008.

[16] C. S. Adamson and M. M. Nevels, “Bright and early: Inhibiting human cytomegalovirus by targeting major immediate-early gene expression or protein function,” *Viruses*, vol. 12, no. 1, 2020.

[17] C. Paulus and M. Nevels, “The human cytomegalovirus major immediate-early proteins as antagonists of intrinsic and innate antiviral host responses,” *Viruses*, vol. 1, no. 3, pp. 760–779,

2009.

[18] S. Omoto and E. S. Mocarski, “Transcription of True Late (2) Cytomegalovirus Genes Requires UL92 Function That Is Conserved among Beta- and Gammaherpesviruses,” *J. Virol.*, vol. 88, no. 1, pp. 120–130, 2014.

[19] H. Gruffat, R. Marchione, and E. Manet, “Herpesvirus late gene expression: A viral-specific pre-initiation complex is key,” *Front. Microbiol.*, vol. 7, no. JUN, pp. 1–15, 2016.

[20] L. Dupont and M. B. Reeves, “Europe PMC Funders Group Cytomegalovirus latency and reactivation : Recent insights into an age old problem,” vol. 26, no. 2, pp. 75–89, 2017.

[21] B. Slobedman, J. L. Stern, A. L. Cunningham, A. Abendroth, D. A. Abate, and E. S. Mocarski, “Impact of Human Cytomegalovirus Latent Infection on Myeloid Progenitor Cell Gene Expression,” *J. Virol.*, vol. 78, no. 8, pp. 4054–4062, 2004.

[22] C. J. Baldick and T. Shenk, “Proteins associated with purified human cytomegalovirus particles.,” *J. Virol.*, vol. 70, no. 9, pp. 6097–6105, 1996.

[23] R. M. Smith, S. Kosuri, and J. A. Kerry, “Role of human cytomegalovirus tegument proteins in virion assembly,” *Viruses*, vol. 6, no. 2, pp. 582–605, 2014.

[24] R. Tandon and E. S. Mocarski, “Viral and host control of cytomegalovirus maturation,” *Trends Microbiol.*, vol. 20, no. 8, pp. 392–401, Aug. 2012.

[25] K. Virologie and D.- Erlangen, “The Two Major Structural Phosphoproteins (pp65 and ppl50) of Human Cytomegalovirus and Their Antigenic Properties,” pp. 1327–1337, 1987.

[26] J. C. Alwine, “The Human Cytomegalovirus Assembly Compartment : A Masterpiece of Viral Manipulation of Cellular Processes That Facilitates Assembly and Egress,” vol. 8, no. 9, pp. 1–4, 2012.

[27] P. Spearman and P. Spearman, “Viral interactions with host cell Rab GTPases Viral interactions with host cell Rab GTPases,” vol. 1248, 2018.

[28] S. V. Indran and W. J. Britt, “A Role for the Small GTPase Rab6 in Assembly of Human Cytomegalovirus,” *J. Virol.*, vol. 85, no. 10, pp. 5213–5219, 2011.

[29] B. Bogdanow *et al.*, “Human cytomegalovirus tegument protein pp150 acts as a cyclin A2-CDK-dependent sensor of the host cell cycle and differentiation state,” *Proc. Natl. Acad. Sci.*, vol. 110, no. 43, pp. 17510–17515, 2013.

[30] J. D. Oduro, R. Uecker, C. Hagemeier, and L. Wiebusch, “Inhibition of Human Cytomegalovirus Immediate-Early Gene Expression by Cyclin A2-Dependent Kinase Activity,” *J. Virol.*, vol. 86, no. 17, pp. 9369–9383, 2012.

[31] H. Weisbach, C. Schablowsky, B. Vetter, I. Gruska, C. Hagemeier, and L. Wiebusch, “Synthetic lethal mutations in the cyclin A interface of human cytomegalovirus,” *PLoS Pathog.*, vol. 13, no. 1, pp. 1–15, 2017.

[32] S. Terhune *et al.*, “Human Cytomegalovirus UL38 Protein Blocks Apoptosis,” *J. Virol.*, vol. 81, no. 7, pp. 3109–3123, 2007.

[33] Z. Q. Yamei Sun, Qunchao Bao, Baoqin Xuan, Wenjia Xu, Deng Pan, Qi Li, “Human Cytomegalovirus Protein pUL38 Prevents Premature Cell Death by Binding to Ubiquitin-Specific Protease 24 and Regulating Iron Metabolism,” vol. 92, no. 13, pp. 1–17, 2018.

[34] N. Yang *et al.*, “Artesunate Induces Cell Death in Human Cancer Cells via Enhancing Lysosomal Function and Lysosomal Degradation of Ferritin *,” vol. 289, no. 48, pp. 33425–33441, 2014.

[35] Z. Qian, B. Xuan, N. Gualberto, and D. Yu, “The Human Cytomegalovirus Protein pUL38 Suppresses Endoplasmic Reticulum Stress-Mediated Cell Death Independently of Its Ability To Induce mTORC1 Activation ,” vol. 85, no. 17, pp. 9103–9113, 2011.

[36] J. A. Isler, A. H. Skalet, and J. C. Alwine, “Human Cytomegalovirus Infection Activates and Regulates the Unfolded Protein Response,” *J. Virol.*, vol. 79, no. 11, pp. 6890–6899, Jun. 2005.

[37] K. P. Malabanan, P. Kanellakis, A. Bobik, and L. M. Khachigian, “Activation Transcription Factor-4 Induced by Fibroblast Growth Factor-2 Regulates Vascular Endothelial Growth Factor-A Transcription in Vascular Smooth Muscle Cells and Mediates Intimal Thickening in Rat Arteries Following Balloon Injury,” pp. 378–387, 2008.

[38] C. McKinney, C. Perez, and I. Mohr, “Poly(A) binding protein abundance regulates eukaryotic translation initiation factor 4F assembly in human cytomegalovirus-infected cells.,” *Proc. Natl. Acad. Sci. U. S. A.*, vol. 109, no. 15, pp. 5627–32, Apr. 2012.

[39] W. A. Bresnahan and T. E. Shenk, “UL82 virion protein activates expression of immediate early viral genes in human cytomegalovirus- infected cells,” vol. 97, no. 26, 2000.

[40] R. F. Kalejta, J. T. Bechtel, and T. Shenk, “Human Cytomegalovirus pp71 Stimulates Cell Cycle Progression by Inducing the Proteasome-Dependent Degradation of the Retinoblastoma Family of Tumor Suppressors,” vol. 23, no. 6, pp. 1885–1895, 2003.

[41] Y. Fu *et al.*, “Human Cytomegalovirus Tegument Protein UL82 Article Human Cytomegalovirus Tegument Protein UL82 Inhibits STING-Mediated Signaling to Evade Antiviral Immunity,” *Cell Host Microbe*, vol. 21, no. 2, pp. 231–243, 2017.

[42] X. Cai, Y. Chiu, and Z. J. Chen, “Review The cGAS-cGAMP-STING Pathway of Cytosolic DNA Sensing and Signaling,” *Mol. Cell*, vol. 54, no. 2, pp. 289–296, 2014.

[43] J. Trgovcich, C. Cebulla, P. Zimmerman, and D. D. Sedmak, “Human Cytomegalovirus Protein pp71 Disrupts Major Histocompatibility Complex Class I Cell Surface Expression,” vol. 80, no. 2, pp. 951–963, 2006.

[44] J. Hesse, S. Ameres, K. Besold, S. Krauter, A. Moosmann, and B. Plachter, “Suppression of CD8+ T-cell recognition in the immediate-early phase of human cytomegalovirus infection,” *J. Gen. Virol.*, vol. 94, no. PART2, pp. 376–386, 2013.

[45] T. I. Arnon *et al.*, “Inhibition of the NKp30 activating receptor by pp65 of human cytomegalovirus,” *Nat. Immunol.*, vol. 6, no. 5, pp. 515–523, 2005.

[46] E. Vivier, E. Tomasello, M. Baratin, T. Walzer, and S. Ugolini, “Functions of natural killer cells,” *Nat. Immunol.*, vol. 9, no. 5, pp. 503–510, 2008.

[47] D. E. Levy, I. J. Marié, and J. E. Durbin, “to Viral Infection,” vol. 1, no. 6, pp. 476–486, 2012.

[48] E. E. Marshall and A. P. Geballe, “Multifaceted evasion of the interferon response by cytomegalovirus,” *J. Interf. Cytokine Res. Off. J. Int. Soc. Interf. Cytokine Res.*, vol. 29, no. 9, pp. 609–619, Sep. 2009.

[49] D. A. Abate, S. Watanabe, and E. S. Mocarski, “Major Human Cytomegalovirus Structural Protein pp65 (ppUL83) Prevents Interferon Response Factor 3 Activation in the Interferon Response,” *J. Virol.*, vol. 78, no. 20, pp. 10995–11006, Oct. 2004.

[50] M. Chevillotte *et al.*, “Major Tegument Protein pp65 of Human Cytomegalovirus Is Required for the Incorporation of pUL69 and pUL97 into the Virus Particle and for Viral Growth in Macrophages ,” vol. 83, no. 6, pp. 2480–2490, 2009.

[51] S. S. Terhune, J. Schröer, and T. Shenk, “RNAs Are Packaged into Human Cytomegalovirus Virions in Proportion to Their Intracellular Concentration,” *J. Virol.*, vol. 78, no. 19, pp. 10390–10398, 2004.

[52] S. M. Varnum *et al.*, “Identification of Proteins in Human Cytomegalovirus (HCMV) Particles : the HCMV Proteome †,” vol. 78, no. 20, pp. 10960–10966, 2004.

[53] S. Michelson *et al.*, “Human cytomegalovirus carries serine/threonine protein phosphatases PP1 and a host-cell derived PP2A,” *J. Virol.*, vol. 70, no. 3, pp. 1415–1423, Mar. 1996.

[54] M. Hakki and A. P. Geballe, “Cellular serine/threonine phosphatase activity during human cytomegalovirus infection,” *Virology*, vol. 380, no. 2, pp. 255–263, Oct. 2008.

[55] A. Bononi *et al.*, “Protein kinases and phosphatases in the control of cell fate,” *Enzyme Res.*, vol. 2011, no. 1, 2011.

[56] J. Jin and T. Pawson, “Modular evolution of phosphorylation-based signalling systems,” *Philos. Trans. R. Soc. B Biol. Sci.*, vol. 367, no. 1602, pp. 2540–2555, 2012.

[57] A. Takai, M. Eto, K. Hirano, and K. Takeya, “Protein phosphatases 1 and 2A and their naturally occurring inhibitors : current topics in smooth muscle physiology and chemical biology,” *J. Physiol. Sci.*, vol. 68, no. 1, pp. 1–17, 2018.

[58] Z. Kónya *et al.*, “Inhibition of protein phosphatase-1 and -2A by ellagitannins : structure-inhibitory potency relationships and influences on cellular systems,” *J. Enzyme Inhib. Med. Chem.*, vol. 34, no. 1, pp. 500–509, 2019.

[59] J. Yu, T. Deng, and S. Xiang, “Structural basis for protein phosphatase 1 recruitment by glycogen-targeting subunits,” *FEBS J.*, vol. 285, no. 24, pp. 4646–4659, 2018.

[60] W. Peti, A. C. Nairn, and R. Page, “Structural basis for protein phosphatase 1 regulation and specificity,” *FEBS J.*, vol. 280, no. 2, pp. 596–611, Jan. 2013.

[61] P. R. Andreassen, F. B. Lacroix, E. Villa-Moruzzi, and R. L. Margolis, “Differential subcellular localization of protein phosphatase-1 α, γ1, and δ isoforms during both interphase and mitosis in mammalian cells,” *J. Cell Biol.*, vol. 141, no. 5, pp. 1207–1215, 1998.

[62] G. MacLeod *et al.*, “PPP1CC2 can form a kinase/phosphatase complex with the testis-specific

proteins TSSK1 and TSKS in the mouse testis," *Reproduction*, vol. 147, no. 1, pp. 1–12, 2014.

[63] H. Ceulemans and M. Bollen, "Functional Diversity of Protein Phosphatase-1, a Cellular Economizer and Reset Button," *Physiological Reviews*, vol. 84, no. 1. pp. 1–39, Jan-2004.

[64] M. Ferreira, M. Beullens, M. Bollen, and A. Van Eynde, "BBA - Molecular Cell Research Functions and therapeutic potential of protein phosphatase 1 : Insights from mouse genetics ☆," *BBA - Mol. Cell Res.*, vol. 1866, no. 1, pp. 16–30, 2019.

[65] A. Manuscript, "The extended PP1 toolkit : designed to create specificity," vol. 35, no. 8, pp. 450–458, 2011.

[66] M. S. Choy, T. M. Moon, R. Ravindran, J. A. Bray, L. C. Robinson, and T. L. Archuleta, "SDS22 selectively recognizes and traps metal-deficient inactive PP1," 2019.

[67] A. Hendrickx *et al.*, "Docking Motif-Guided Mapping of the Interactome of Protein Phosphatase-1," *Chem. Biol.*, vol. 16, no. 4, pp. 365–371, Apr. 2009.

[68] E. Heroes, B. Lesage, J. Görnemann, M. Beullens, L. Van Meervelt, and M. Bollen, "The PP1 binding code: a molecular-lego strategy that governs specificity," *FEBS J.*, vol. 280, no. 2, pp. 584–595, Jan. 2013.

[69] P. Wakula, M. Beullens, H. Ceulemans, W. Stalmans, and M. Bollen, "Degeneracy and Function of the Ubiquitous RV X F Motif That Mediates Binding to Protein Phosphatase-1," *J. Biol. Chem.*, vol. 278, no. 21, pp. 18817–18823, May 2003.

[70] Â. Gergely, D. J. Hartshorne, F. Erdo, È. Kiss, and F. W. Herberg, "Study of the subunit interactions in myosin phosphatase by surface plasmon resonance," vol. 1697, pp. 1687–1697, 2000.

[71] A. S. Pinheiro, J. A. Marsh, J. D. Forman-Kay, and W. Peti, "Structural signature of the MYPT1-PP1 interaction," *J. Am. Chem. Soc.*, vol. 133, no. 1, pp. 73–80, 2011.

[72] M. S. Choy *et al.*, "Understanding the antagonism of retinoblastoma protein dephosphorylation by PNUTS provides insights into the PP1 regulatory code," *Proc. Natl. Acad. Sci. U. S. A.*, vol. 111, no. 11, pp. 4097–4102, 2014.

[73] M. S. Choy *et al.*, "Structural and Functional Analysis of the GADD34 : PP1 eIF2 a Phosphatase," *CellReports*, vol. 11, no. 12, pp. 1885–1891, 2015.

[74] H. P. Harding *et al.*, "Stress-Induced Gene Expression in Mammalian Cells," vol. 6, pp. 1099–1108, 2000.

[75] W. Shi *et al.*, "GADD34–PP1c recruited by Smad7 dephosphorylates TGF type I receptor," pp. 291–300, 2002.

[76] E. Heroes *et al.*, "Structure-Guided Exploration of SDS22 Interactions with Protein Phosphatase PP1 and the Splicing Factor BCLAF1," *Structure*, vol. 27, no. 3, pp. 507-518.e5, 2019.

[77] A. K. T. Signaling, "Protein Phosphatase 1 Regulatory Subunit SDS22 Inhibits Breast Cancer Cell Tumorigenesis by Functioning as a Negative Regulator," *Neoplasia*, vol. 21, no. 1, pp. 30–40, 2019.

[78] G. Khoudoli, “Sds22 regulates aurora B activity and microtubule-kinetochore interactions at mitosis,” no. May, 2014.

[79] A. Eiteneuer, J. Seiler, M. Weith, M. Beullens, and B. Lesage, “Inhibitor- 3 ensures bipolar mitotic spindle attachment by limiting association of SDS 22 with kinetochore-bound protein phosphatase - 1,” no. January 2015, 2014.

[80] M. Rojas, G. Vasconcelos, and T. E. Dever, “An eIF2α-binding motif in protein phosphatase 1 subunit GADD34 and its viral orthologs is required to promote dephosphorylation of eIF2α,” *Proc. Natl. Acad. Sci.*, vol. 112, no. 27, pp. E3466–E3475, Jul. 2015.

[81] M. Tyagi *et al.*, “Reactivation of latent HIV - 1 provirus via targeting protein phosphatase - 1,” *Retrovirology*, pp. 1–17, 2015.

[82] T. Ammosova *et al.*, “Nuclear Targeting of Protein Phosphatase-1 by HIV-1 Tat Protein *,” vol. 280, no. 43, pp. 36364–36371, 2005.

[83] T. Ammosova *et al.*, “Protein Phosphatase-1 Activates CDK9 by Dephosphorylating Ser175,” vol. 6, no. 4, 2011.

[84] T. Ammosova *et al.*, “Expression of a protein phosphatase 1 inhibitor, cdNIPP1, increases CDK9 threonine 186 phosphorylation and inhibits HIV-1 transcription,” *J. Biol. Chem.*, vol. 286, no. 5, pp. 3798–3804, Feb. 2011.

[85] N. Kumari, Y. Saygideger, A. Kulkarni, and M. Jerebtsova, “Inhibition of HIV-1 infection in humanized mice and metabolic stability of protein phosphatase-1-targeting small molecule 1E7-03 Inhibition of HIV-1 infection in humanized mice and metabolic stability of protein phosphatase-1-targeting small molecule,” no. February 2018, 2017.

[86] D. Cougot *et al.*, “Inhibition of PP1 phosphatase activity by HBx: A mechanism for the activation of hepatitis B virus transcription,” *Sci. Signal.*, vol. 5, no. 205, 2012.

[87] P. A. Ilinykh *et al.*, “Role of protein phosphatase 1 in dephosphorylation of Ebola virus VP30 protein and its targeting for the inhibition of viral transcription,” *J. Biol. Chem.*, vol. 289, no. 33, pp. 22723–22738, 2014.

[88] A. Katic, “MASTERARBEIT / MASTER ’ S THESIS,” 2019.

[89] X. Li, M. Wilmanns, J. Thornton, and M. Köhn, “Elucidating human phosphatase-substrate networks,” *Sci. Signal.*, vol. 6, no. 275, p. rs10, May 2013.

[90] F. J. J. Rieder *et al.*, “Human cytomegalovirus phosphoproteins are hypophosphorylated and intrinsically disordered,” *J. Gen. Virol.*, vol. 98, no. 3, pp. 471–485, Mar. 2017.

[91] Y. Cavignac *et al.*, “The Cellular Proteins Grb2 and DDX3 Are Increased upon Human Cytomegalovirus Infection and Act in a Proviral Fashion,” *PLoS One*, vol. 10, no. 6, p. e0131614, Jun. 2015.

[92] S. Nekhai, M. Jerebtsova, A. Jackson, and W. Southerland, “Author Index To Volume 4,” *Curr. HIV Res.*, vol. 5, no. 1, pp. iii–iii, 2006.

[93] H. Jin, Z. Yan, Y. Ma, Y. Cao, and B. He, “A Herpesvirus Virulence Factor Inhibits Dendritic Cell

Maturation through Protein Phosphatase 1 and I B Kinase," *J. Virol.*, vol. 85, no. 7, pp. 3397–3407, 2011.

[94] J. A. Jadwin, M. Ogiue-Ikeda, and K. MacHida, "The application of modular protein domains in proteomics," *FEBS Lett.*, vol. 586, no. 17, pp. 2586–2596, 2012.

[95] J. Wang, A. Alekseenko, D. Kozakov, and Y. Miao, "Improved Modeling of Peptide-Protein Binding Through Global Docking and Accelerated Molecular Dynamics Simulations," *Front. Mol. Biosci.*, vol. 6, no. October, pp. 1–10, 2019.

[96] C. McKinney, J. Zavadil, C. Bianco, L. Shiflett, S. Brown, and I. Mohr, "Global Reprogramming of the Cellular Translational Landscape Facilitates Cytomegalovirus Replication," *Cell Rep.*, vol. 6, no. 1, pp. 9–17, Jan. 2014.

[97] L. Q. Hong-Brown, C. R. Brown, D. S. Huber, and C. H. Lang, "Lopinavir impairs protein synthesis and induces eEF2 phosphorylation via the activation of AMP-activated protein kinase," *J. Cell. Biochem.*, vol. 105, no. 3, pp. 814–823, 2008.

[98] H. A. Vincent, B. Ziehr, and N. J. Moorman, "Human Cytomegalovirus Strategies to Maintain and Promote mRNA Translation.," *Viruses*, vol. 8, no. 4, p. 97, Apr. 2016.

[99] M. A. Rowland, B. Harrison, and E. J. Deeds, "Article Phosphatase Specificity and Pathway Insulation in Signaling Networks," *Biophysj*, vol. 108, no. 4, pp. 986–996, 2015.

[100] J. F. Díaz-villanueva, R. Díaz-molina, and V. García-gonzález, "Protein Folding and Mechanisms of Proteostasis," pp. 17193–17230, 2015.

[101] B. De Chassey, L. Meyniel-schicklin, J. Vonderscher, P. André, V. Lotteau, and U. De Lyon, "Virus-host interactomics : new insights and opportunities for antiviral drug discovery Influenza virus," pp. 1–14, 2014.

[102] M. Chevillotte *et al.*, "Major Tegument Protein pp65 of Human Cytomegalovirus Is Required for the Incorporation of pUL69 and pUL97 into the Virus Particle and for Viral Growth in Macrophages," *J. Virol.*, vol. 83, no. 6, pp. 2480–2490, 2009.

[103] L. B. Thackray *et al.*, "Critical Role for Interferon Regulatory Factor 3 (IRF-3) and IRF-7 in Type I Interferon-Mediated Control of Murine Norovirus Replication," *J. Virol.*, vol. 86, no. 24, pp. 13515–13523, 2012.

[104] M. Gu *et al.*, "Protein phosphatase PP1 negatively regulates the Toll-like receptor- and RIG-I-like receptor-triggered production of type I interferon by inhibiting IRF3 phosphorylation at serines 396 and 385 in macrophage," *Cell. Signal.*, vol. 26, no. 12, pp. 2930–2939, Dec. 2014.

[105] H. Duan *et al.*, "Phosphorylation of PP1 regulator Sds22 by PLK1 ensures accurate chromosome segregation," *J. Biol. Chem.*, vol. 291, no. 40, pp. 21123–21136, 2016.

[106] N. Goodacre, P. Devkota, E. Bae, S. Wuchty, and P. Uetz, "Seminars in Cell & Developmental Biology Protein-protein interactions of human viruses," vol. 99, pp. 31–39, 2020.